Article:
Xu, H., Pope, I., Gupta, V. et al. (12 more authors) (2022) Large-scale compartment fires to develop a self-extinction design framework for mass timber—Part 1: Literature review and methodology. Fire Safety Journal, 128. 103523. ISSN 0379-7112

https://doi.org/10.1016/j.firesaf.2022.103523

Fire Safety Journal 128 (2022) 103523

Contents lists available at ScienceDirect

Fire Safety Journal

journal homepage: www.elsevier.com/locate/firesaf

Large-scale compartment fires to develop a self-extinction design framework for mass timber—Part 1: Literature review and methodology

Hangyu Xu [a], Ian Pope [a], Vinny Gupta [a], Jaime Cadena [a], Jeronimo Carrascal [a], David Lange [a], Martyn S. McLaggan [a], Julian Mendez [a], Andrés Osorio [a], Angela Solarte [a], Diana Soriguer [a], Jose L. Torero [b], Felix Wiesner [a,c], Abdulrahman Zaben [a], Juan P. Hidalgo [a,*]

[a] The University of Queensland, School of Civil Engineering, St Lucia, QLD, Australia
[b] University College London, Department of Civil, Environmental & Geomatic Engineering, UK
[c] The University of Edinburgh, School of Engineering, UK

ARTICLE INFO

Keywords:
Performance-based design
Compartment fires
Heat transfer
Protection of wood
Large-scale
Cross-laminated timber
Mass timber

ABSTRACT

Fire safety remains a major challenge for engineered timber buildings. Their combustible nature challenges the design principles of compartmentation and structural integrity beyond burnout, which are inherent to the fire resistance framework. Therefore, self-extinction is critical for the fire-safe design of timber buildings.

This paper is the first of a three-part series that seeks to establish the fundamental principles underpinning a design framework for self-extinction of engineered timber. The paper comprises: a literature review introducing the body of work developed at material and compartment scales; and the design of a large-scale testing methodology which isolates the fundamental phenomena to enable the development and validation of the required design framework.

Research at the material scale has consolidated engineering principles to quantify self-extinction using external heat flux as a surrogate of the critical mass loss rate, and mass transfer or Damköhler numbers. At the compartment scale, further interdependent, complex phenomena influencing self-extinction occurrence have been demonstrated. Time-dependent phenomena include encapsulation failure, fall-off of charred lamellae and the burning of the movable fuel load, while thermal feedback is time-independent. The design of the testing methodology is described in reference to these fundamental phenomena.

1. Introduction

Timber structures are increasingly being incorporated into modern medium and high-rise buildings due to their appealing aesthetics and sustainability credentials [1]. Engineered timber products have resolved many of the structural limitations and reduced the natural constraints associated with solid sawn timber. As a result, engineered timber elements comprising cross-laminated timber (CLT) and glued-laminated timber (Glulam) have emerged as a popular trend in modern construction. Mass timber structures have also been shown to provide value related to ease of construction [2] and deconstruction in favour of a Circular Economy [3]. When using CLT for slabs and walls, and Glulam for beams and columns, construction can be achieved within shorter periods on-site and with less noise and dust pollution.

Given the advantages of timber construction and the strong push towards reducing embodied carbon in construction that will be required to achieve the 2015 UN Sustainable Development Goals (SDG) [4], there is an expectation that the number of timber medium and high-rise buildings will increase significantly. Timber construction can primarily benefit aspects related to SDG Goals 9, 11, 12, and especially Goal 13 associated with combating climate change. However, fire safety remains a primary, strong constraint for the use of engineered timber in tall buildings.

Fire safety design principles for tall buildings rely on 'fire resistance' as a means of ensuring the integrity and stability of compartmentation and the stability of the structure beyond the burnout of the movable fuel load present within the compartment [5]. The movable fuel load traditionally refers to items such as furnishings. Compartmentation is intended to constrain the vertical and horizontal spread of the fire beyond the compartment of origin into multiple building spaces and

* Corresponding author.
E-mail address: j.hidalgo@uq.edu.au (J.P. Hidalgo).

https://doi.org/10.1016/j.firesaf.2022.103523
Received 5 July 2021; Received in revised form 11 November 2021; Accepted 2 January 2022
Available online 3 January 2022

floor levels. Structural stability is required to ensure that the building will not collapse—an essential goal during the evacuation of building occupants and fire brigade intervention and property protection. This is particularly relevant to medium to high-rise buildings where the characteristic times for evacuation and intervention can exceed the potential characteristic times for structural collapse.

Among the many assumptions embedded in the 'fire resistance' approach is that the fire will burn out once the movable fuel load has been fully consumed. An increase in the fuel load will challenge the performance assessment approach used for compartmentation and structural stability since the time required to achieve burnout will be increased. The combustible nature of mass timber means that it may continue to burn after the movable fuel load has burned out. This therefore poses an additional and as yet unquantified risk to achieving compartmentation and structural stability.

To overcome this, the most common design approach to date for multiple mass timber medium and high-rise buildings has been based on the use of encapsulation (e.g. the Brock Commons Tallwood House in Vancouver, the Monterey Kangaroo Point in Brisbane, the Forté building in Melbourne or the Mjøstårnet in Brumunddal). The intent behind this approach is to be able to use the conventional 'reaction-to-fire' (e.g. Ref. [6]) and 'fire-resistance' (e.g. Ref. [7]) frameworks established for non-combustible structures. This approach has also made it into prescriptive solutions in building codes; e.g. the Building Code of Australia (BCA) [8], based on the work led by Forest and Wood Products Australia [9] or the 2018 and 2021 International Building Code (IBC) [10,11] and International Fire Code (IFC) [12] changes in the USA [13], which allow the use of mass timber structures for buildings with limited height and with an encapsulation system, such as fire-rated plasterboard. The premise of this approach is that if the timber does not pyrolyse, the hazards posed by exposed mass timber structures are mitigated. These hazards include the contribution to the fire growth (heat release rate), the continued reduction of strength caused by increased heating and loss of cross-section, more severe external flaming and the continuous burning of the structure [14,15]. Therefore, the approach relies on compliance by delivering a method that can be deemed equivalent to the solutions used for non-combustible materials. Other prescriptive approaches with a less conservative approach can be found, e.g. the 2020 Canadian National Building Code that allows partial exposure of CLT based on a series of demonstrator tests [16,17].

Building height restrictions and fire protection specifications vary substantially depending on the region, and regularly change as building codes are updated based on ongoing research. In the US, timber buildings were limited to 85 ft (25.9 m) according to the 2015 IBC [18]. However, since the latest 2021 IBC [10,11], timber buildings are permitted to be constructed up to 270 ft (82.3 m) in height if protected with non-combustible protections. In contrast, in Australia, buildings exceeding 25 m are required to be designed using a performance-based approach to allow the use of mass timber. Timber buildings of less than 25 m can be designed using a prescriptive (Deemed-to-Satisfy) approach if encapsulation and sprinklers are used [8,9]. In Europe, building height restrictions for using timber as loading bearing elements or exposed linings vary from country to country [19].

Whereas these changes in prescriptive requirements might be deemed to provide a path forward for mass timber structures in the built environment, encapsulating mass timber reduces some of the benefits of timber construction, e.g. appealing aesthetics, environmental benefits, or construction speed. In addition, this introduces uncertainties and possible risks associated with craftmanship and complex system behaviour.

There are also examples of buildings with exposed timber structures, i.e. with no encapsulation (e.g. 25 King Street, Brisbane), developed in recent years thanks to the application of holistic yet conservative design approaches where the risks of mass timber construction are addressed explicitly. Law and Hadden [20] emphasised that a key aspect to consider when designing mass timber structures is to design for the cessation of burning (flaming self-extinction) of the timber structures after the burnout of the movable fuel load. This condition is vital for a fire safety strategy relying on compartmentation and structural stability.

When considering the cessation of burning of the mass timber structure, emphasis is mainly drawn on flaming combustion rather than smouldering combustion for multiple reasons. Continuous self-sustained flaming of timber structures induces larger heat fluxes within the compartment; hence the thermal degradation rates of the structure may be orders of magnitude greater compared to smouldering combustion. While smouldering extinction of flat surfaces of most wood species is expected to occur under no external heating conditions [21], smouldering is expected to occur in areas with limited heat losses, such as within joints, natural gaps or insulated areas. This can lead to a structural collapse in significantly longer time scales (e.g. 29 h after the onset of heating as shown in Ref. [22]). The larger time scales associated with the smouldering hazard should therefore not be neglected in design. However, they offer a wide margin period for adequate management strategies by fire and rescue services.

Multiple institutions have undertaken extensive research programmes, explicitly and implicitly, on the flaming self-extinction of CLT in the last decade. Three different approaches can be identified: (1) small-scale research aimed at investigating the fundamental aspects influencing self-extinction; (2) large-scale research tests conducted to reveal complex system behaviour only observable at a realistic scale; and (3) large-scale test demonstrations to justify code amendments that provide a prescriptive pathway for mass timber. All three approaches can contribute to developing engineering tools for the design and realisation of mass timber buildings. The third approach has been shown to provide a faster pathway to CLT implementation in buildings. However, it is at the risk of lacking a holistic understanding of mass timber performance under fire conditions and failing to adequately address the uncertainties and risks associated with the system behaviour. The first two approaches can incrementally contribute to an advanced scientific understanding of the performance of CLT under fire conditions that enables an optimisation of the fire safety strategy. However, research using these approaches often included limitations such as the lack of loading conditions for the structural timber or the use of compartment dimensions not representative of actual compartment sizes built throughout the world, which could influence the self-extinction behaviour of CLT in compartments. Despite the efforts by the fire safety engineering community, the research to date has not produced a consolidated design framework for CLT self-extinction. This is attributed to the complexity of this phenomenon, with multiple factors influencing its occurrence in compartment fires.

Given that the fire safety strategy relies on burnout, it is critical that self-extinction must be considered in the design of mass timber buildings. The critical factors affecting self-extinction need to be identified, and the state-of-the-art knowledge at the material scale needs to be incorporated at the compartment scale to be able to achieve this. From this, a consolidated framework based on fundamentals can be developed, which enables verifiably safe and confident usage of mass timber.

2. Aim

The aim of the study is to present fundamental principles underpinning the development of a framework aimed at delivering engineered timber self-extinction by design. This paper presents a review of existing literature on the subject and a methodology to enable the formulation and validation of a self-extinction design framework. The objective of the literature review is to identify the critical phenomena influencing the self-extinction of CLT by focusing on seminal sources. The methodology consists of a large-scale experimental campaign using compartment fire tests where these critical factors are then isolated from one another.

3. Review of flaming self-extinction research on solid wood and mass timber structures

3.1. Material scale

Literature on the burning behaviour of wood is dense [23,24] and findings regarding its ability to stop burning under specific critical conditions date back to early studies by Bamford *et al.* [25]. In the 1970s, Tewarson and Pion [26] and Petrella [27] identified that the heat generated by the flame of certain solid materials such as wood can be lower than the surface heat losses. Therefore, the resulting energy balance is insufficient for flaming combustion to self-sustain without the presence of an external heat source. Today, the ability of wood to stop burning is generally denoted as self-extinction, which can be described by the fire point theory postulated by Rasbash et al. [28]. The fire point theory states that the burning process of a condensed fuel cannot be sustained if a sufficient mass flux of pyrolysates is not provided to the flame (gas-phase reaction zone). The mass flux of pyrolysates combined with the air flow structure defines the flame temperature and thus the viability of the combustion reactions to proceed. This concept is the same as the critical Damköhler number for flame extinction, commonly used in the combustion community [29]. This principle is used implicitly in the fire science community, with the focus on the mass transfer of pyrolysates because the flow field can generally be considered invariable [30]. For that reason, a non-dimensional mass transfer (B) number is generally used to define the critical condition of extinction. Initially proposed by Spalding [31] to describe the energy surface boundary condition for the burning of liquid droplets and later further developed for solids by Torero et al. [32] to properly quantify heat losses based on the work by Emmons [33], the mass transfer number represents the ratio between the energy available and that required to pyrolyse the fuel. In the combustion of wood, the heat flux from the flame imposed on the pyrolysis front is dampened by the growing char layer, leading to a condition where $B < 1$ and flaming extinction by quenching occurs. Consistent with the findings of Tewarson and Pion [26] and Petrella [27], the self-sustained combustion of wood can occur through an external heat source imposed onto the surface to raise the mass transfer number such that $B > 1$ [34]. Since the rate of generation of pyrolysates ($\dot{m}''_p$) is dependent on the heat balance in the pyrolysis region (solid--phase reaction zone), the problem has often been simplified to the study of the condensed phase and the thermal boundary condition.

Recently, Bartlett et al. [35] and Emberley et al. [36] used bench-scale experiments to verify the existence of a critical mass loss rate for self-extinction ($\dot{m}''_{cr}$) for Cross-Laminated Timber made of softwood (Spruce and European spruce, *Picea abies*) as 3.5 ± 0.3 g/m^{2}s and 3.9 ± 0.4 g/m^{2}s, respectively without a forced external air flow. Emberley et al. [37] further identified the critical mass loss rate for various timber species, including Radiata Pine (3.7 ± 0.2 g/m^{2}s), Red Ironbark (7.2 g/m^{2}s), Balsa (8.3 ± 1.9 g/m^{2}s), Kumaru (5.1 ± 0.6 g/m^{2}s) and Blackbutt (2.7 ± 0.5 g/m^{2}s). Using redwood timber, Arnórsson et al. [38] further verified the critical mass loss rate increases proportionally with the square of the flow velocity, consistent with a critical Damköhler number analysis. This suggests that a quiescent external flow condition provides a conservative quantity from an engineering perspective, thus reinforcing the invariable flow structure assumption.

The critical rate of mass loss, which depends on the wood species, is associated with the surface mass flux of pyrolysates ($\dot{m}''_p$) generated within the pyrolysis region below the char, the surface mass flux of water vapour generated within the unpyrolysed timber ($\dot{m}''_w$), and the mass loss of char through oxidation at the surface ($\dot{m}''_c$). Once the char region is formed, the mass flux of pyrolysates released at the surface depends on the energy balance established in a hypothetically thin pyrolysis region located in between the char layer and the dried timber (refer to Fig. 1). Assuming that the pyrolysis region develops under isothermal conditions as in Ref. [39] (i.e. the pyrolysis reaction is dominated by heat transfer rather than kinetics), the energy balance at the pyrolysis region can be defined as:

$$\dot{m}''_p = \frac{\dot{q}''_{c\to p} - \dot{q}''_{p\to d}}{\Delta H_p} \tag{1}$$

where $\dot{q}''_{c\to p}$ is the heat flux at the interface between char and pyrolysis regions ($x = x_p$), $\dot{q}''_{p\to d}$ is the heat flux at the interface between the pyrolysis region and the dried timber, and ΔH_p is the heat of pyrolysis. The heat flux entering the pyrolysis region is determined by the heat transfer within the char region, which can be formulated as:

$$\dot{q}''_e + \dot{q}''_{fl} - \dot{q}''_{loss} = -k_c \left.\frac{\partial T}{\partial x}\right|_{x=0} \tag{2}$$

$$\frac{\partial}{\partial x}\left(k_c \frac{\partial T}{\partial x}\right) = \rho_c c_c \frac{\partial T}{\partial t} + \dot{q}'''_{c,ox} \tag{3}$$

$$-k_c \left.\frac{\partial T}{\partial x}\right|_{x=x_p} = \dot{q}''_{c\to p} \tag{4}$$

where $\dot{q}''_e$ and $\dot{q}''_{loss}$ are the external heat flux and heat losses to the environment at the surface of the char ($x = 0$), $\dot{q}''_{fl}$ is the radiative and convective heat flux from the flame, k_c and $\rho_c c_c$ are the thermal conductivity and volumetric heat capacity of the char, and $\dot{q}'''_{c,ox}$ is the heat generated by the oxidation reaction, determined by the oxygen diffused into the char layer. If the char layer is approximated as a thermally thin element and the diffusion of oxygen into the char is neglected, the en-

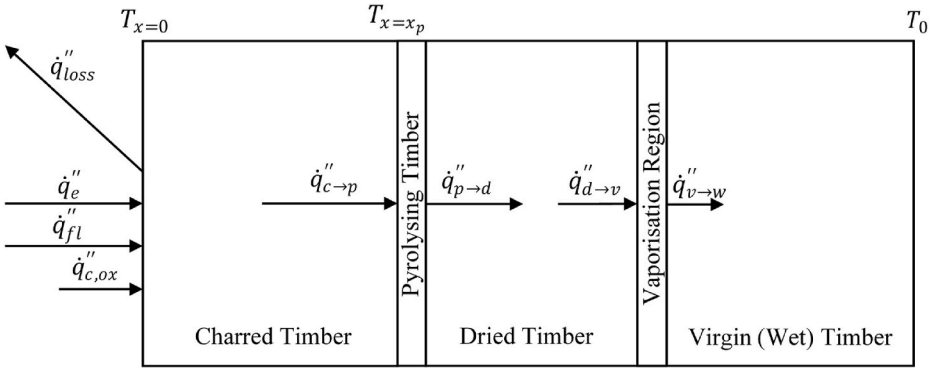

Fig. 1. Schematic showing the different regions of timber under quasi-steady-state burning conditions: charred timber, pyrolysing timber, dried timber, vaporisation region and virgin (wet) timber. $\dot{q}''_{c\to p}$, $\dot{q}''_{p\to d}$, $\dot{q}''_{d\to v}$ and $\dot{q}''_{v\to w}$ represent the heat flux between charred timber, pyrolysing timber, dried timber, vaporisation layer and virgin (wet) timber. T_0 is the initial temperature.

ergy balance proposed by Emberley et al. [36] and Cuevas et al. [40] holds as:

$$\dot{q}''_{c\rightarrow p} = \dot{q}''_{e} + \dot{q}''_{fl} - \dot{q}''_{loss} + \dot{q}''_{c,ox} - \frac{dq''}{dt} \quad (5)$$

where $\dot{q}''_{c,ox}$ is the heat produced by the oxidation of the char (assumed to take place at the char surface where a maximum mass fraction of oxygen is available), and $\frac{dq''}{dt}$ is the temporal change of heat per unit area in the char (transient energy term). As described by Emberley et al. [36], for thick timber samples exposed to a constant external heat flux, a quasi-steady state is reached in the burning rate after a transient period of nearly 10 min. The thickness consideration is a key factor related to a semi-infinite solid behaviour, thus the back boundary condition does not affect the heat transfer [41]. Reaching a quasi-steady burning rate indicates that a quasi-steady energy balance can be assumed in the control volumes defined by the pyrolysis and char regions. Therefore, the transient term, $\frac{dq''}{dt}$, must approximate zero and, in fact, the heat transfer in the char region cannot be defined using a lumped capacitance approach (thermally thin) but as a steady conduction heat transfer (thermally thick), where the volume (thickness) of the char is the cause of the reduction in heat flux experienced at the interface char-pyrolysis region. The quasi-steady condition implies that the pyrolysis and oxidation fronts progress steadily at similar rates, allowing for an approximately constant char thickness (d_c). Therefore, the energy balance shall be described considering a steady gradient in the char layer:

$$\dot{q}''_{c\rightarrow p} = k_c \frac{T_{x=0} - T_{x=x_p}}{d_c} = \dot{q}''_{e} + \dot{q}''_{fl} + \dot{q}''_{c,ox} - \dot{q}''_{loss} \quad (6)$$

where and $T_{x=0}$ and $T_{x=x_p}$ are the temperatures at the surface of the char and the temperature at the pyrolysis front. Equations (1) and (6) show a linear relationship between the pyrolysis rate and the external heat flux, suggesting that a critical heat flux ($\dot{q}''_{e,cr}$) can be associated with a critical pyrolysis rate ($\dot{m}''_{p,cr}$).

The quasi-steady thermal and burning behaviour experienced by wood under steady external heating conditions has been generally proven experimentally by presenting the mass loss rate per unit area (e.g. Ref. [36]). Unfortunately, experimental demonstration of the quasi-steady energy balance remains a crude analysis due to the lack of high-density in-depth temperature measurements and thermocouple conduction error.

Results extracted from the wood oxidative pyrolysis model developed by Lautenberger and Fernandez-Pello [42] can be used to supplement the limitations of the experimental information. The model results allow extracting a more detailed description of the evolution of isotherms representative of pyrolysis and water vaporisation, and thermal gradients in different regions. Fig. 2 shows model results for a 100 mm thick wood element using the model parameters from Ref. [42] exposed to 40 kW/m^2. The location and speed over time of isotherms 100 °C and 300 °C (Fig. 2a), representing the vaporisation and pyrolysis processes, clearly indicate a transient period in the first 5–10 min followed by a quasi-steady behaviour, as observed experimentally by Emberley et al. [36]. Additionally, the thermal gradients in the char and dried regions show minor variability over time after 10 min (Fig. 2b), thus confirming the quasi-steady thermal behaviour. The dampening of the heat flux into the pyrolysis front (Eq. (4)), often attributed to the low conductivity of char, is not strictly due to the different conductivity in dried wood and char but the volume (thickness) of char, which results in a significant thermal gradient.

Bartlett et al. [35] and Emberley et al. [37] experimentally validated the concept of a critical heat flux for self-extinction using European spruce. After a characteristic time, the external heat flux at the surface of the char can be used as a surrogate variable to define a bound (critical value) under which flaming extinction occurs. However, they identified different values due to differences in the experimental methodology (~31 kW/m^2 and 43.6 ± 4.7 kW/m^2, respectively). Cuevas et al. [40] identified that self-extinction has a stochastic nature, influenced by the testing conditions used. They further identified that self-extinction of flaming combustion on the charred surface of *Pinus radiata* occurs within a range of external heat flux, with the minimum value being 30 kW/m^2 and the maximum value 40 kW/m^2 at a 21% oxygen concentration atmosphere. This surrogate offers a powerful simplification for fire engineering practice, as it removes a significant level of complexity associated with modelling wood pyrolysis.

3.2. Compartment scale

The dense body of work at the bench scale has provided an understanding of major fundamental mechanisms resulting in the flaming self-extinction of wood. However, the fire dynamics of a compartment are modified by the introduction of exposed engineered timber, which means that consideration only on a material scale is not viable to resolve self-extinction.

In the last decade, multiple research institutions, including the University of Edinburgh, The University of Queensland, the National Institute of Standards and Technology (NIST), the National Research Council of Canada (NRC), the Research Institutes of Sweden (RISE), CERIB and Carleton University, have led several fire tests of CLT compartments at different scales and geometrical configurations [16, 43–49]. Most of these tests relate to quasi-cubic 'small compartments' with limited ventilation, more representative of residential construction than 'open-plan compartments' with extensive ventilation typically found in commercial and office buildings. The focus on the former is justified as the first step in complexity and a more conservative scenario for self-extinction from a thermal feedback perspective due to the restricted ventilation conditions. Even in non-combustible compartments, there is still a poor understanding of open plan fire dynamics. Open plan timber compartments represent an especially difficult and

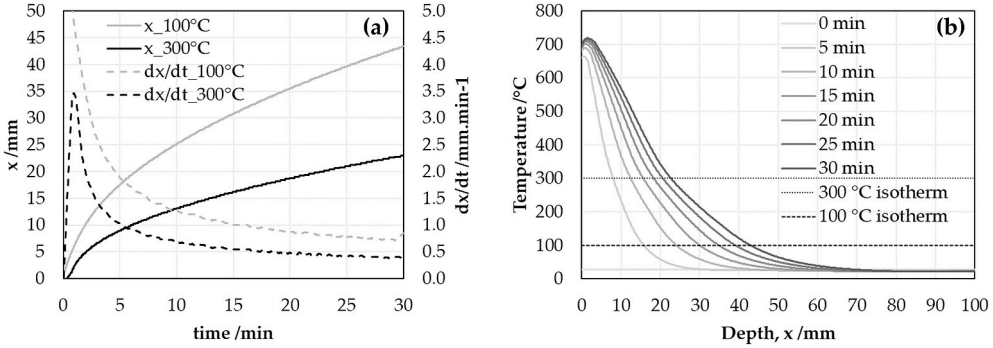

Fig. 2. Outcomes from a Gpyro simulation on a wood sample burning under steady-state conditions [42]. (a) Evolution of the 100 °C and 300 °C isotherms positions and their temporal derivative over time. (b) Thermal gradient for different time steps.

complex scenario, with increasing efforts being developed to understand these complexities [49].

The combined body of work on 'small compartments' with limited ventilation has identified multiple layers of complexity in the interactions between exposed engineered timber and the compartment that can affect the occurrence of flaming self-extinction. These complexities include thermal feedback between surfaces, increased burning due to char fall-off and failure of encapsulation, and variation in the nature and density of the fuel load. Compartment fire experiments identifying parameters determining these complexities are discussed in detail.

3.2.1. Thermal feedback

Using *Pinus radiata* CLT compartments of reduced scale (internal dimensions 0.48 m × 0.48 m and 0.37 m), Gorska [50] demonstrated that self-extinction can be achieved if the thermal feedback from the compartment boundaries (external heat flux) after burnout drops below the threshold defined for the same timber species by Emberley et al. (45 ± 1 kW/m^2) [46]. After burnout, the magnitude of the external heat flux was shown to decay at a different rate depending on the ratio of exposed timber (i.e. the more timber exposed, the slower the decay). For specific compartment geometries, a critical ratio of exposure could be reached, where a steady heat flux above the critical value is maintained, and steady burning of the timber could eventually be achieved.

On a large scale, Bartlett et al., Emberley et al., Su et al. and Wiesner et al. [16,17,22,44,46] have demonstrated that, under specific conditions, self-extinction of exposed CLT can also occur in real-scale compartments. The studies by Bartlett et al. [44] and Emberley et al. [46] hypothesised that, given a compartment geometry, a critical ratio of exposed surface area of timber defines a criterion for self-extinction. Consistent with the findings by Gorska [50], an increased ratio of exposed timber to the surface area of the compartment boundaries (A_{CLT}/A_T), representing energy generation, and reduced ratio of opening area (A_o/A_T), representing energy losses, can lead to sustained flaming of the CLT due to the enhanced thermal feedback.

In addition, Gorska [50] identified that the problem is not only dominated by the ratio of surfaces (i.e. simply a radiative exchange between surfaces in an optically thin medium) but by the pyrolysis rate from the CLT surfaces. Gorska demonstrated that for compartments with exposed CLT, those with an exposed timber ceiling would achieve similar decay and extinction conditions than those without. This reveals the importance of further considering the combustion dynamics and smoke accumulation in the compartment to assess the resulting incident heat flux (irradiation) on the combustible surfaces.

3.2.2. Char fall-off

Besides the success in demonstrating the critical link between thermal feedback and self-extinction at the compartment scales, the experiments developed by Hadden et al. [51] further demonstrated that other time-dependent factors, including the fall-off of charred lamellae and encapsulation failure, can also influence and prevent CLT self-extinction.

Char fall-off of CLT is defined herein as a bond failure between charred lamella and the lamella beneath (charred or not). Char fall-off may be caused by the degradation of the adhesive between lamellae at elevated temperatures [52]. The fall-off of cracked, charred timber pieces occurs gradually throughout the compartment from exposed CLT surfaces and results in the exposure of uncharred (or mildly charred) timber to the fire. This phenomenon has been shown to enhance the burning rate of timber in several experiments [36,46,51,53], resulting in the increase of heat release rate in the compartment. Char that has fallen onto the floor can also behave as an additional fuel source, thus contributing to continued burning and an increase in the total heat released. Due to the laminated nature of CLT, the process of char fall-off may repeat itself, thereby preventing self-extinction from happening [41].

Char fall-off is highly dependent on the thermal stability and capacity of the glue to ensure proper adhesion between lamellae, amongst other factors. Polyurethane-based and melamine formaldehyde adhesives are commonly used in CLT to enable rapid manufacturing [53]. These adhesives may experience a reduction in adhesion or cohesion performance at temperatures below char formation. Polyurethane adhesives cover a wide range of applications, and the performance under heat may vary significantly [54]. Previous research has shown that char fall-off can be affected by the loading conditions [55], and it may be delayed with the use of more thermally stable adhesives [17,52,53].

Char fall-off is a thermo-mechanical process that involves the system characteristics, the properties of its components (adhesive, timber, char), and the loads the system is subjected to Ref. [56]. Differences in the chemical formulation of the adhesive can lead to differences in the underlying chemical decomposition, which is expected to result in a different fall-off performance. Whether char fall-off can be prevented entirely still requires a thorough understanding of the thermo-mechanical conditions under which engineered timber is exposed. Multiple studies have shown that the shear strength retention at elevated temperatures varies significantly between different adhesive types [57–59] and within different adhesive formulations of the same type [60]. Multiple recent studies have shown that reduced adhesive bonding at elevated temperatures will reduce the overall load-bearing capacity of timber before visible char fall-off occurs [61–63]. Even if a more robust solution can be found using high-performance CLT where char fall-off could be entirely prevented, it is a priority to identify potential performance criteria to allow design and optimisation of common CLT using ordinary adhesives.

3.2.3. Encapsulation failure

Encapsulation failure refers to the integrity and insulation failure of passive fire protection materials (fireproofing) attached to the surface of the timber. As with timber frame construction, fire-rated plasterboard is currently the most used encapsulation system for mass timber [64], although other less common encapsulation systems, e.g. intumescent coatings [65] and calcium silicate boards [66], are increasingly receiving interest for use on mass timber. Integrity failure of the encapsulation—understood as the mechanical detachment—leads to further timber exposure in the compartment. Exposure to an increased ratio of unprotected timber promotes continuous burning of the timber surfaces, thus can lead to a critical thermal feedback condition under which extinction may not be achieved.

On the basis of an approach to design that relies on encapsulation, plasterboard fall-off (integrity failure) may be considered an indicator of failure. However, an adequate performance criterion to identify the failure of the encapsulation is likely related to the onset of pyrolysis of the timber substrate (insulation failure). Once encapsulated timber reaches a pyrolysis temperature, char will form. The formation of char might promote mechanical failure and allow sufficient oxygen to approach the char surface, making combustion possible. The criterion based on a critical temperature has been proposed in performance-based methodologies to use combustible insulation safely [67], and following this approach, a similar temperature criterion has been proposed for encapsulated timber delivering an alternative form of 'fire resistance' rating (k_i rating [68]). Furthermore, this approach is present in prescriptive codes, such as the Building Code of Australia, to ensure that timber walls can be argued to perform equivalently to inert materials [9].

3.2.4. Fuel load

The aforementioned subjects have been the primary focus of research in recent years. In contrast, the impact of the nature and density of fuel load on self-extinction has attracted little explicit attention. The fuel load density, defined as the total thermal energy that can be released per floor unit area (MJ/m^2), is a basic design parameter used in structural fire engineering that determines the fire duration [69]. Historically,

wood cribs have been the most common source of fuel used in compartment fire research. Examples are the work developed by Thomas and Heselden [70] in the development of the *Compartment Fire Framework* [71], where burnout is determined based on fuel load density and burning rates of wooden cribs; or the work by Magnusson and Thelandersson on the "Swedish fire curves" [72], or the parametric time-temperature curves [73,74] implemented in the Eurocodes [75], where temperature-time curves are determined as a function of the fuel load density and the opening factor. The use of wood cribs as fuel load in fire testing has been adopted throughout modern times as a condensed fuel with a predictable burning behaviour. For instance, wood cribs were also used to develop the experimental work for the *Natural Fire Safety Concept* [76] that gave way to Eurocode methods for the analysis of structural safety in case of fire [75,77] and by most of the more recent research focused on open-plan compartments fire dynamics [78].

Several researchers have opted to use wood cribs to test mass timber construction [17,22,44,46,51,79], whereas others have opted for fuel loads consisting of furniture more representative of actual conditions [16,80–82], or even controlled gas burners [47,83]. The work of Harmathy in the 1970s on small compartment fires [84,85] showed that fuels of varying mass transfer (B) numbers have a strong influence on the compartment fire dynamics. The distinct role of fuels of different nature in compartment fires is not a novel insight. However, recent research in the context of timber buildings [50,86] has demonstrated that the fuel load can influence CLT self-extinction. This influence is manifested by the burnout time, heat flux severity and the decay phase in a compartment fire. Given that the burnout time and the fire's decay phase can heavily dictate the self-extinction of timber, the choice of fuel load nature for testing mass timber structures needs to be revisited.

3.3. Summary of knowledge gaps towards a self-extinction design framework

As previously introduced, an essential design principle for the fire safety strategy of mass timber buildings relates to attaining burnout of the movable fuel load followed by self-extinction, before compartmentation and structural stability are compromised. To date, the most comprehensive conceptual guide available to address self-extinction by design is the discussion provided by Law and Hadden [20]. However, despite the research efforts on particular parameters affecting the self-extinction of CLT, there is not a well-defined framework available to address design for self-extinction based on a systematic testing campaign that identifies each failure mode in isolation.

Self-extinction has been studied at a material scale and identified critical conditions, but the extent of applicability to compartments is not yet fully understood. Systematic testing on the thermal feedback conditions has been presented for reduced size compartment experiments [50]. For full-size compartments, the mechanisms necessary to determine self-extinction are however limited by the scaling process in terms of fire dynamics (i.e. flow fields and radiation determining the fire boundary condition and burning behaviour of the fuel load) and thermo-mechanical behaviour of the CLT and encapsulation (i.e. char fall-off and encapsulation failure). Testing performed at these scales has generally focused on defining specific design parameters and evaluating the outcome of the mechanisms inhibiting self-extinction. This has not been done parametrically, so the effect of each mechanism cannot be isolated and evaluated. These mechanisms include time-dependent phenomena such as:

- **burning of the movable fuel**: determined by the fuel nature, quantity and configuration, and the ventilation conditions, and can trigger the thermo-mechanical degradation of the engineered timber and the encapsulation;
- **char fall-off**: determined by the engineered timber properties and the fire exposure, and which leads to direct exposure of subsequent lamellae and an increased feedback of incident heat flux to the timber surfaces due to the additional fuel source on the floor; and
- **encapsulation failure**: determined by the encapsulation properties and the fire exposure, and which leads to an increased feedback of incident heat flux to the timber surfaces due to the additional exposure of timber;

whereas the time-independent phenomenon refers to:

- **thermal feedback within the compartment after the movable fuel burnout**: determined by the geometric characteristics of the compartment and ventilation, and the configuration of exposed and encapsulated timber surfaces, which combined define the incident heat flux onto the timber surfaces.

Given the complexity and interdependency of these phenomena, there is a need to consolidate and validate a self-extinction design framework by performing large-scale tests in which each of these mechanisms can be verified in isolation where possible. Such a testing methodology must capture the relevant phenomena influencing the occurrence of self-extinction to enable the validation process. Due to the multiple parameters affecting these phenomena (i.e. characteristics of the compartment and opening geometry, engineered timber, encapsulation, and exposure of timber), conservative assumptions need to be made when selecting test parameters, informed by a fundamental understanding of the problem.

4. Methodology

4.1. Rationale for the design of the testing programme

The methodology used to formulate and validate the self-extinction framework is inspired by the quantitative analysis process that designers would need to apply to assess the occurrence of self-extinction. However, this methodology replaces the quantitative analysis with well-controlled, parametric large-scale tests (demonstrators) to isolate the occurrence of each failure mechanism. The use of large-scale tests resolves scaling issues but restricts the number of tests that can effectively be executed due to time and economic constraints. A dense level of instrumentation is used to quantify and describe the outcomes in the most explicit manner possible, resolving the spatial distribution of multiple quantities key to describing fire dynamics and self-extinction phenomena. The key parameters to be quantified in the study of CLT self-extinction in compartment fires are:

i. Characteristic time for burnout of the movable fuel load (t_{bo}).
ii. Characteristic time for the occurrence of char fall-off ($t_{f,c}$).
iii. Characteristic time for the occurrence of encapsulation failure ($t_{f,e}$).
iv. Characteristic thermal feedback within the compartment after burnout ($\dot{q}''_{e,decay}$).

Given the time-dependency of the encapsulation and char fall-off failures, a key consideration for the design and development of these tests is to be able to control the characteristic time for burnout of the movable fuel load (t_{bo}). A re-filling pool fire system is proposed to control the burnout duration, similar to the one described in Ref. [87]. This approach is novel compared to previous systematic experimental work on CLT compartments using condensed fuels in which the fuel load is fixed based on characteristic design values. Using this approach, the complexity associated with burnout of solids fuels can be removed, and demonstration scenarios can be produced such that failure mechanisms are either induced ($t_{bo} > max(t_{f,c}, t_{f,e})$) or prevented ($t_{bo} < min(t_{f,c}, t_{f,e})$) under rapid-onset severe post-flashover conditions. In order to understand the upper bound of the characteristic time to reach these failure

modes, the selection of CLT is based on maximising the thickness of the first lamella. The selection of encapsulation is based on the standard practice requirements for fire-protected timber in the Building Code of Australia [9].

The characteristic thermal feedback depends on the parameters A_o/A_T and A_{CLT}/A_T. Similar to previous research undertaken by Hadden et al. [51] and Gorska [50], the thermal feedback is then assessed by varying the initial exposure of CLT and fixing the opening area (e.g. exposing two or three surfaces of CLT). However, it is necessary first to establish a scenario where time-dependent failure mechanisms can be prevented where possible. This can be done by controlling the burnout duration based on an understanding of the characteristic time for char fall-off and plasterboard failures to occur.

Finally, to address the impact of fuel nature on self-extinction, a charring fuel with a lower mass transfer (B) number is used to compare with a self-extinction test in which a liquid fuel with a higher mass transfer (B) number is used. The key consideration for this analysis is to use the same fuel load (in equivalent MJ) in either case.

To complete such a validation study, a series of six large-scale tests was developed. The following list provides a brief description of major design considerations for the proposed test matrix. A visual representation of the test matrix is provided in Fig. 3. Specific details regarding the experimental setup are provided in subsequent sub-sections.

- **Encapsulation study**: Test 1.1 and Test 1.2 correspond to compartments where the CLT is fully encapsulated, as shown in Fig. 7a. The intent of these tests is to assess the time-scale condition for encapsulation failure and the nature of that failure (i.e. whether it is an insulation or an integrity failure). For that purpose, the burnout duration is controlled such that Test 1.1 experiences failure (higher fuel load scenario) and Test 1.2 does not experience encapsulation failure (lower fuel load scenario).
- **Char fall-off study**: Test 2.1 and Test 2.2 correspond to compartments where a lateral wall (left wall looking from the door) and the ceiling are exposed CLT, and the other surfaces are encapsulated, as shown in Fig. 7b. This configuration has in the past demonstrated the ability to achieve self-extinction if time-dependent failures are avoided [46]. The intent of these tests is to assess the time-scale condition for char fall-off to occur. For that purpose, the burnout duration is controlled such that Test 2.1 experiences char fall-off (higher fuel load that ultimately leads to loss of compartmentation) and Test 2.2 does not experience char fall-off (lower fuel load that subsequently leads to self-extinction).
- **Thermal feedback study**: Test 3.1 corresponds to a compartment where the two lateral walls and the ceiling are exposed CLT, while the other surfaces are encapsulated, as shown in Fig. 7c. Test 3.1 is set up such that the movable fuel load consumed is equivalent to that in Test 2.2. In combination with Test 2.2, the intent of these two tests is to assess the thermal feedback condition for which self-extinction does not occur.
- **Fuel load nature study**: Test 4.1 corresponds to a compartment where a lateral wall and the ceiling are exposed CLT, and the other surfaces are encapsulated (like Test 2.2), as shown in Fig. 7d. The movable fuel corresponds to a wood crib with a fuel load (in MJ) equivalent to the fuel load consumed in Test 2.2. The intent of these tests is to assess the impact of fuel load nature on self-extinction.

4.2. Cross-laminated timber

The cross-laminated timber panels used to construct the compartments were manufactured by XLam. The CLT corresponded to CL3/125 [88], composed of three lamellae of 45-35-45 mm thick *Pinus radiata* with a measured mean density of 485 kg m^{-3} (nominal density of 500 kg m^{-3} according to the manufacturer). The thickest possible outer lamella was selected so that the response of the CLT to a long fire duration could be analysed, thus reducing the potential for early char fall-off. The CLT lamellae were glued using Purbond HBS polyurethane adhesive. The mean moisture content of CLT throughout the testing programme was 10–14%.

4.3. Compartment characteristics

The external dimensions of the compartment were 3.4 m × 3.4 m × 3.125 m, which was defined by transportation restrictions for panels without joints. All adjacent CLT panels were connected using Rothoblaas® HBS 8 × 220 wood screws at a spacing of 300 mm. The centrelines of the screws were located 62.5 mm from the edge of the top CLT panel through the centre of the middle lamella of the overlaid perpendicular CLT panel. The compartment had a single opening of external dimensions 0.85 m × 2.40 m. Internally, a false floor was constructed so that instrumentation and the fuel pipes of the burner system or the load cells would not be affected by the heat from the fire. The distance from the top surface of the false floor to the ground was 0.3 m. The internal

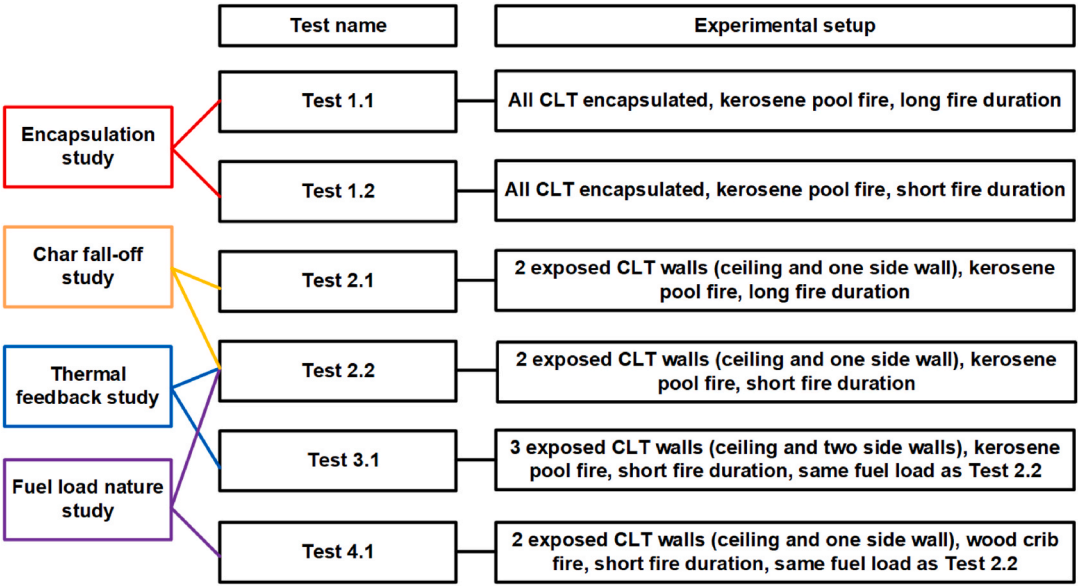

Fig. 3. Diagram showing the test series and the related studies of the factors influencing self-extinction.

dimensions of the compartment were 3.15 m × 3.15 m × 2.70 m, and the dimensions of the opening were 0.85 m × 2.10 m due to the height of the false floor. Depending on the configuration used, the resulting inverse opening factor ($A_T/A_0\sqrt{H_o}$) was in the range 17.2–17.6 $m^{-1/2}$ (encapsulation thickness considered), defined as the ratio of the area of the internal compartment surface area excluding the floor (A_T) to the ventilation factor. The ventilation factor is the product of the opening area (A_0) and the square-root of the opening height (H_o), resulting in $A_0\sqrt{H_o} = 2.38\ m^{5/2}$. An overview of the compartment is shown in Fig. 4.

The false floor consisted of a timber frame system made of, from top to bottom, 2 × 50 mm Rockwool® RockTech S 400 (Tests 1.1 and 1.2) or 4 × 25 mm Rockwool® Conlit (remainder of tests), 13 mm thick Knauf FireShield plasterboard, 10 mm chipboard or medium-density fibreboard, and 70 × 35 mm timber joists. The false floor system was similar in design to those used in previous studies [51,89]. Besides the protection offered to the instrumentation underneath, the stone wool insulation provided a conservative thermal boundary condition (nearly adiabatic).

4.4. Fire source

4.4.1. Pool fire system

For the studies focused on the time-scale and thermal feedback conditions (Tests 1.1, 1.2, 2.1, 2.2 and 3.1), the objective of the methodology was to control the time to burnout. Therefore, a solid fuel was not considered because the supply of fuel had to be controlled. Instead, kerosene (with a net heat of combustion of 44.1 MJ/kg) was selected as the fuel source for the fire—a high combustibility ratio (large B number) and non-charring fuel. The selection of this fuel was also based on the outcomes from earlier studies [50,86] that demonstrated a relatively fast time to reach flashover and a fast decay phase compared to charring fuels. These features allowed for easy identification of the exact fuel burnout time and reduced uncertainty in CLT self-extinction due to the omission of smouldering char on the floor. A gas burner system was discarded due to the low soot yield and the absence of thermal feedback controlling the fuel load burning rate. The fuel supply to the compartment was controlled using a bespoke re-filling tray system, similar in concept to the one described in Ref. [87].

The pool fire system consisted of a connected vessel arrangement in which the surface of the pool fire was allowed to remain at an approximately constant level for the duration of the fire. The internal component was a 1.0 m × 1.0 m × 0.1 m stainless steel tray placed within the compartment, whereas the external vessel was a tub that received fuel from an IBC tank using a float (buoy) valve. During the fire, the kerosene being burned inside the compartment was replaced with kerosene from the external tub. Under steady conditions, kerosene flowed from the main IBC tank into the external tub using the float system, thus replenishing the burned kerosene from the tray in the compartment. A flow meter was used to measure the flow from the IBC tank to the external tub. When it was decided to induce burnout, a valve between the external tub and the internal tray was shut off, leading to burnout approximately 12 min later when the remaining fuel in the tray was consumed. The schematics of the system are shown in Fig. 5.

In order to ensure that the tray of the pool fire did not buckle excessively due to thermal expansion, and that the heat losses from the pool fire could be quantified for future energy balance analyses, the tray was also equipped with a cooling system. The tray was manufactured as a hollow double-skin tray, with a 6 mm internal void acting as a cooling water jacket, through which a flow of water of approximately 50 L/min at ambient temperature was forced. The temperature of the water flow before entering and after leaving the tray were monitored.

The dimensions of the tray system (1 m × 1 m) were chosen to

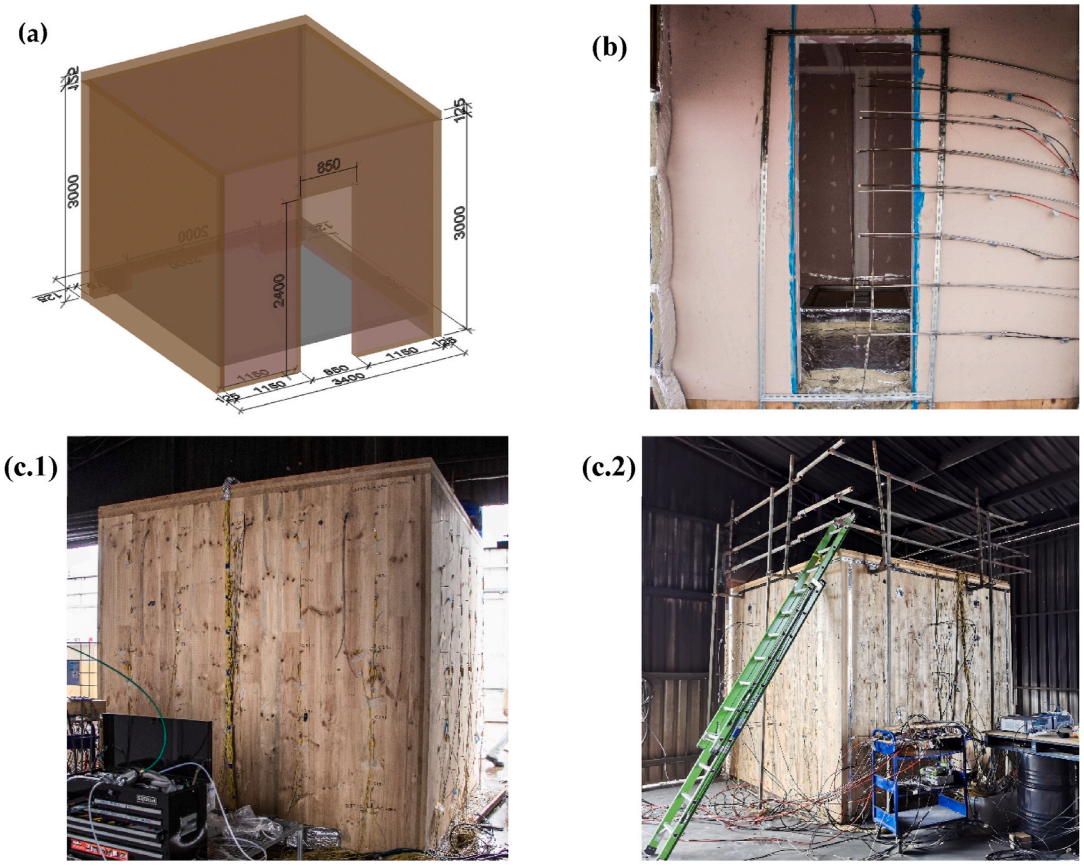

Fig. 4. (a) Schematic 3D drawing of the compartment. (b) External image of the front of the compartment showing the door instrumentation. (c.1-2) External image of the back of the compartment showing CLT instrumentation.

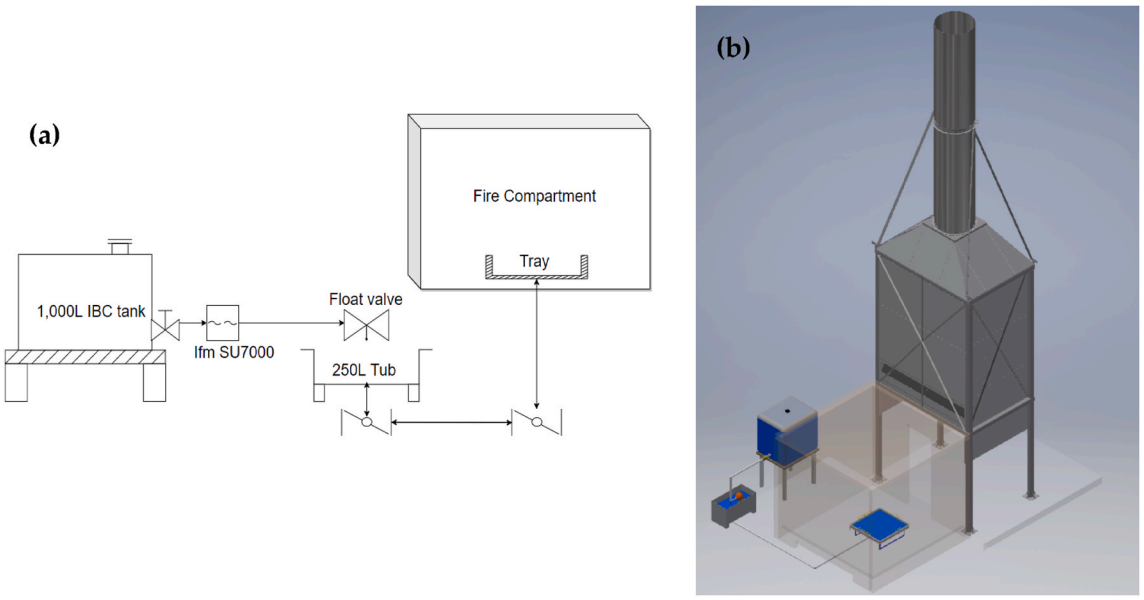

Fig. 5. (a) Diagram showing the pool fire system. (b) 3D schematics of the compartment, pool fire system and the buoyancy calorimeter.

provide a heat release rate sufficient to produce flashover conditions and reach under-ventilated conditions within the compartment. Several calibrations 'free burns' were carried out throughout the testing campaign, in which the fuel was burned directly beneath the hood of the buoyancy calorimeter (described in Section 4.6.1), outside of the compartment. Two series of free burns were conducted with the tray placed on top of a load cell and filled with a different mass of kerosene. Series 1 (lower fuel load, 2 tests) consisted of 16.2–17.2 kg (714.4–758.5 MJ) of fuel, while series 2 (higher fuel load, 3 tests) consisted of 35.9–42.4 kg (1583.2–1869.8 MJ). The mass loss and heat release rate of these free burns are presented in Fig. 6a.

4.4.2. Wood crib

The objective of the methodology for the study of the fuel load nature (Tests 2.2 and 4.1) was to compare the influence on self-extinction of using condensed fuels with dissimilar *B* numbers and decomposition behaviours. For that purpose, a wood crib was built for Test 4.1, using softwood (untreated pine MGP10) sticks with approximate dimensions 1000 mm × 45 mm × 45 mm, a mean density of 569 kg/m^3 and 10% mean moisture content, which was sampled and measured on the same day of the tests using an oven-dry method [90]. Each layer consisted of 11 sticks separated by a gap of approximately 45 mm. A total of 14 layers was used, resulting in a fuel load of 177.5 kg (17.89 kg/m^2 per unit area of compartment floor). The gross heat of combustion of the wood was measured using a bomb calorimeter [91], providing a value of 18.65 MJ/kg. Assuming a net heat of combustion of 17.5 MJ/kg [75], the fuel load of the crib was 3106 MJ (313 MJ/m^2). The mass loss of the wood crib during the test was measured using a load cell placed underneath the false floor platform supporting the crib.

Similar to the calibration tests for the kerosene tray, a free burn of a similar wood crib was undertaken directly beneath the hood of the buoyancy calorimeter. The wood crib with an initial mass of 181.3 kg (3172.8 MJ) and was placed on top of a load cell. The mass loss rate and heat release rate are presented in Fig. 6b.

4.5. Configuration of CLT exposure

For the fully-encapsulated tests (Test 1.1 and Test 1.2), the CLT was protected with two layers of 13 mm thick, paper-faced Knauf Fireshield (10.5 kg/m^2) attached to the CLT with screw fixings. The first layer (inner layer) of plasterboard uses 32 mm long fixings every 400 mm in field (300 mm on the edges). The second layer (exposed) of plasterboard uses 45 mm long fixings every 300 mm in field (200 mm on edges). The fixings were covered with MastaBase, a plaster-based cement for

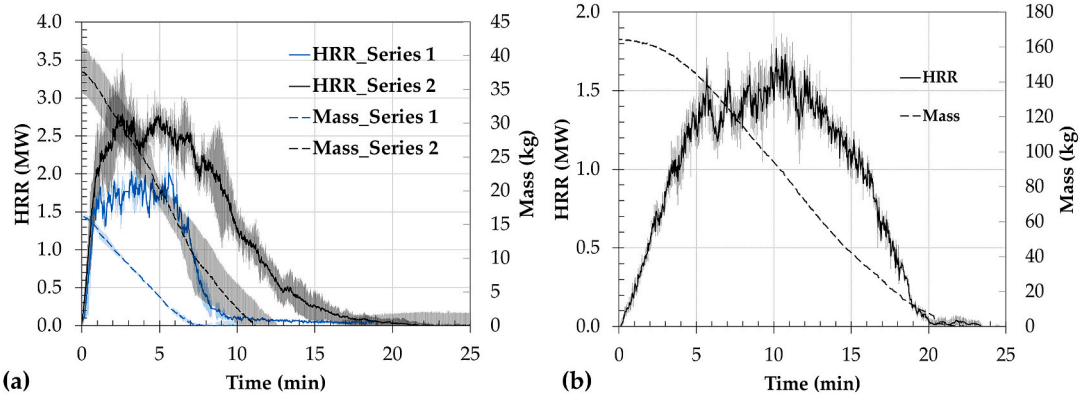

Fig. 6. Mass loss and heat release rate from free burns for (a) Series 1 (714.4–758.5 MJ) and 2 (1583.2–1869.8 MJ) of the kerosene tray and (b) the wood crib (3172.8 MJ). Note: recovery of mass at the end of each kerosene burn is an artefact measurement caused by the cooling of the tray system. The curves show the average of data from each group, with the shaded area shows the variation among different tests within each group.

Fig. 7. Internal images of the compartments showing: (a) Test 1.1 (encapsulation study); (b) Test 2.2, (char fall-off study); (c) Test 3.1 (thermal feedback study); (d) Test 4.1 (fuel load nature study). Compartments shown in (a-c) used an internal 1 m × 1 m pool fire as the fire source, whereas (d) used a 1 m × 1 m wood crib.

bedding tape and plasterboard joints. Test 1.2 included heat flux sensors replacing a portion of the encapsulation, whereas Test 1.1 did not so that it would not influence the mechanism of failure.

Tests with two exposed CLT surfaces (ceiling and lateral wall) included Tests 2.1, 2.2 and 4.1. Test 3.1 included three exposed CLT surfaces (ceiling and two lateral walls). For the tests with lower fuel load (Test 2.2, 3.1 and 4.1), the encapsulation and fixings were the same as the fully-encapsulated compartments.

For the test that used a higher fuel load (Test 2.1), the encapsulation was altered to try to provide a more robust encapsulation system similar to that developed by Hadden et al. [51]. The system consisted of a sandwich system with a 13 mm thick layer of Knauf Fireshield, a 25 mm thick layer of Rockpipe® 650 (128 kg/m^3), and another 13 mm thick layer of Knauf Fireshield. The inner plasterboard layer (directly against

Fig. 8. (a) Buoyancy calorimeter during the experiment. (b) Internal view of the fire obtained with a water-cooled GoPro camera.

the CLT) used 32 mm long fixings every 400 mm in field (300 mm on the edges). The Rockpipe stone wool layer (on the top of the inner layer plasterboard) used 50 mm length timber screws with 16 mm external diameter washers every 300 mm in field The outer plasterboard layer was fixed with 65 mm long screws every 300 mm in field (200 mm on edges). The fixings were covered with MastaBase, and plasterboard joints were covered with MastaBase and plasterboard jointing tape, which made sure that the fixings were protected from direct fire exposure and maximise the integrity of the plasterboard layers.

Fig. 7 shows internal views of the exposure configuration for the four studies.

4.6. Instrumentation

4.6.1. Calorimeter

A distinguishing feature of these tests was the 14 m tall buoyancy-driven calorimeter shown in Figs. 5b and 8a—a modified version of the buoyancy-driven calorimeter developed by the Commonwealth Scientific and Industrial Research Organisation (CSIRO) [92]. The design of this equipment was inspired by the buoyancy-driven calorimeters developed by the Fire Research Station (FRS) to quantify the heat release rate of vehicle fires in a tunnel [93]. The buoyancy-driven calorimeter works using the same principle to quantify heat release as

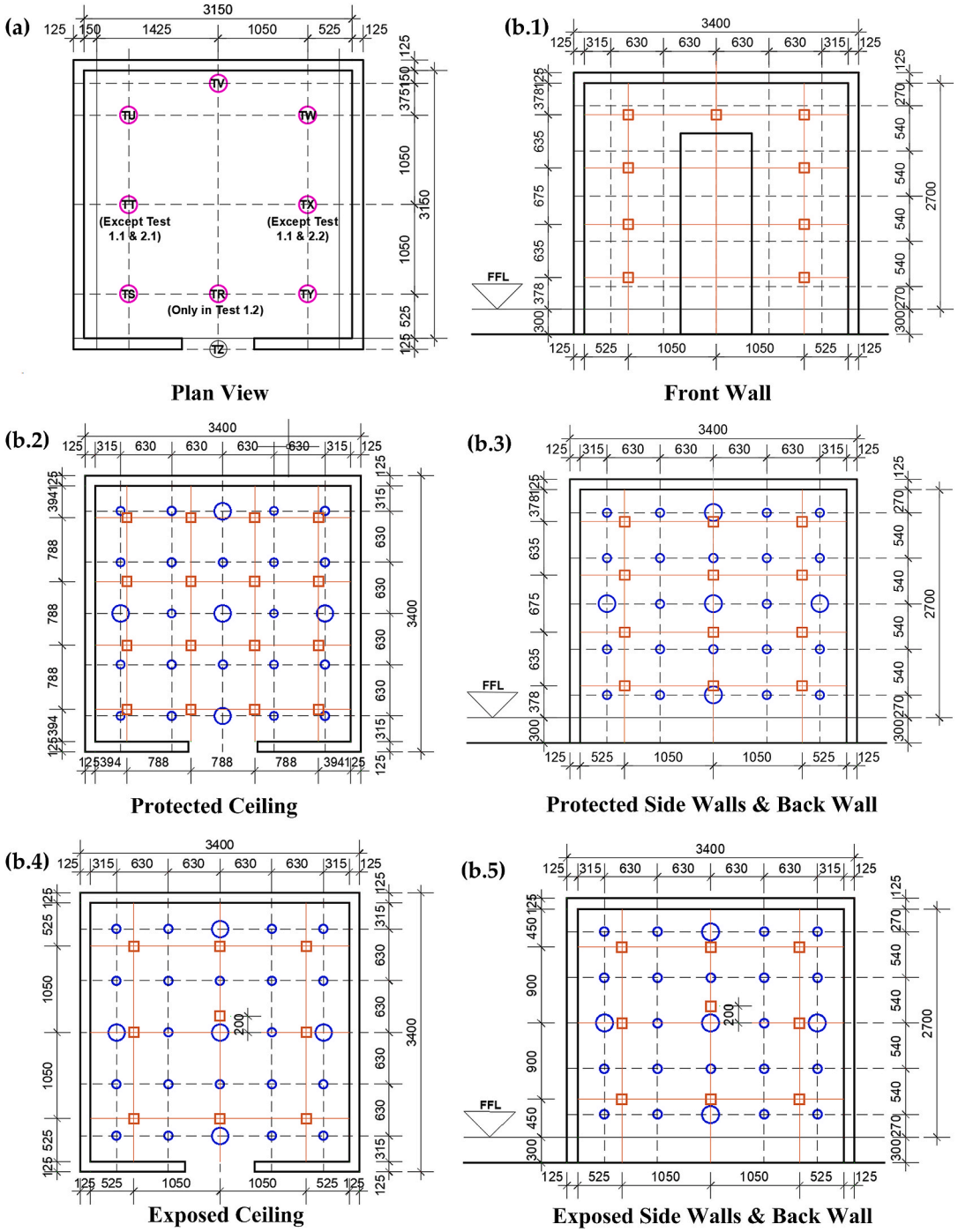

Fig. 9. (a) Locations of gas-phase thermocouple trees (Seven TCs per tree). (b) Locations of in-depth thermocouples (blue circles – small for individual TCs and large for multiple clustered TCs), and thin-skin calorimeters (brown squares). (For interpretation of the references to colour in this figure legend, the reader is referred to the Web version of this article.)

the Cone Calorimeter [94]; however, using buoyancy to channel the exhaust gases rather than a mechanical fan. This feature avoids the need for a heat resistant fan with a large extraction capacity.

This apparatus was located next to the compartment's opening so that the external plume was directed into the buoyancy calorimeter duct. The buoyancy calorimeter was equipped with: two gas analysis sampling points using gas analysers detailed in section 4.6.6, three bi-directional velocity probes and three 1.5 mm K-type thermocouples. These devices were all located 1 m below the top edge of the calorimeter chimney to enable the quantification of the total heat release rate through a species-evolution calorimetry approach (oxygen consumption or carbon dioxide generation) [95]. The calibration of the calorimeter constant was performed using free burns of kerosene pool fires and wood cribs directly underneath the calorimeter, where the mass loss was monitored (refer to section 4.4). Further details of the calorimeter are presented in Ref. [92].

In order to further quantify the internal heat release rate, the opening of the compartment included eight bi-directional velocity probes and corresponding thermocouples at different heights, and sampling points for gas analysis, as shown in Fig. 12a. Details concerning these instruments are described below.

4.6.2. Gas-phase temperature measurements

Internally, the compartment was equipped with thermocouple trees at multiple locations to measure gas-phase temperatures (refer to Fig. 9a). Each tree carried seven thermocouples (TCs) spaced evenly at approximately 338 mm height intervals between the floor and the ceiling. These probes enabled evaluating the gas-phase temperature distributions and the severity of the fire. An additional eight thermocouples (tree TZ Fig. 9a) were paired with the velocity probes in the opening (described in Section 4.6.4) to measure the temperature of gases flowing in and out of the compartment, and to indicate the height of the neutral plane. For Tests 1.1, 1.2, 2.1 and 2.2, all of the gas-phase thermocouples were type K mineral-insulated metal-sheathed (MIMS) thermocouples, with diameters of 1.5 mm. In Tests 3.1 and 4.1, a larger diameter of 3.0 mm was used for greater robustness, as many of the thinner thermocouples were destroyed at high temperatures of more than 1100 °C produced in the earlier tests. In the latter two tests, a type N thermocouple was added to each tree to corroborate the measurements of the type K thermocouples at such high temperatures.

4.6.3. Heat flux sensors

Thin skin calorimeters (TSCs) were installed in walls and ceilings to measure incident radiant heat flux onto the internal surfaces of the compartment boundaries. The intent of these measurements was to quantify the severity of the fire and identify the heating conditions onto the compartment boundaries in the decay phase of the fire after burnout. The TSCs were designed and calibrated according to the methodology presented in Ref. [96]. The TSCs used in this series of tests consisted of 50 mm diameter and 40 mm thick vermiculite cylinders, and a 1 mm thick and 10 mm diameter Inconel disc. Fig. 10 shows the TSCs embedded within the compartment boundaries and the calibration of the C factor for quantification of the incident heat flux. Thin skin calorimeters were not installed in Test 1.1 to prevent any possible damage to the encapsulation system.

A series of three TSC towers were used in each test to measure the heat flux coming from the opening of the compartment. The TSCs were located on the towers as depicted in Fig. 11.a, and the TSC towers were located away from the opening as shown in Fig. 11b. In each tower, three TSCs were installed at heights of 0.4, 0.9 and 1.4 m from the false floor level (FFL). The TSCs were contained inside vermiculite square plates, which were fixed in their positions on a small steel column, while the rest of the steel column was thermally insulated using stone wool. The central tower (T2) was directly in front of the compartment at a distance of 3.6 m. The two side towers were placed on a 2.3 m and 2.4 m radius (T1 and T3, respectively) and at a 45-degree angle on both sides of the centre tower, with the compartment opening centre line as the radius centre.

4.6.4. Velocity probes

Stainless steel bi-directional velocity probes (BDP) were manufactured according to Ref. [97] and installed at the centreline of the opening and within the compartment on the walls (refer to Fig. 12b). The probes were attached to OMEGA PX277-0.1D5V (±10 Pa) and GEMS 5266 (±50 Pa) differential pressure transducers. The probe-transducer assembly was subject to significant errors at low flow velocities consistent with compartment openings, and therefore required calibration [98]. Both transducer models were calibrated following [78]. The locations of 8 velocity probes positioned at the compartment opening are shown in Fig. 12a, the lateral view of probes inside compartment is shown in Fig. 12b, however, ceiling velocity probes were only included in Test 1.2. The number of velocity probes inside compartment varied between different tests. Nine velocity probes were installed internally in Test 1.2 with three probes mounted 300 mm normal to the wall on the ceiling, the back wall and one of the lateral walls. Velocity probes were not installed in Test 1.1 to prevent damage to the encapsulation system. Six velocity probes were installed internally in Test 2.1, 2.2, 3.1 and 4.1, with 3 probes on the back wall and 3 on one

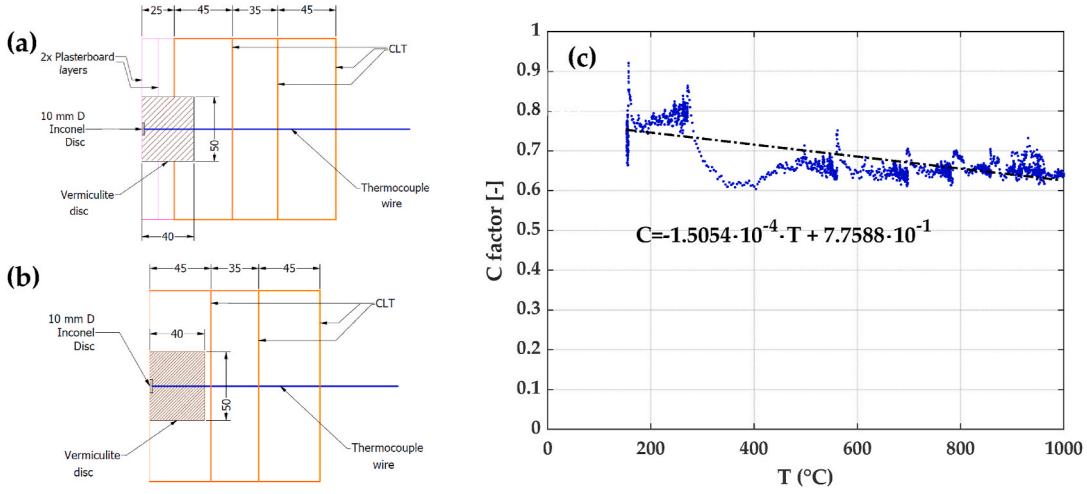

Fig. 10. View of the TSC embedded on (a) encapsulated and (b) exposed CLT. (c) C-factor for the TSCs calibrated using a radiant panel system at The University of Queensland.

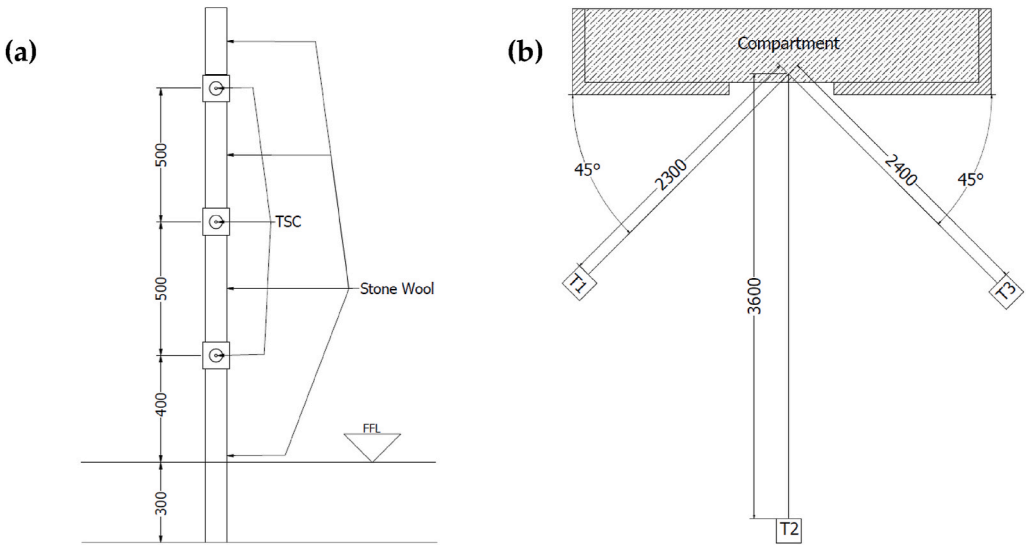

Fig. 11. (a) Front view of the externally located TSC towers with three TSCs in height. (b) Location of the TSC towers with respect to the compartment opening (plan view).

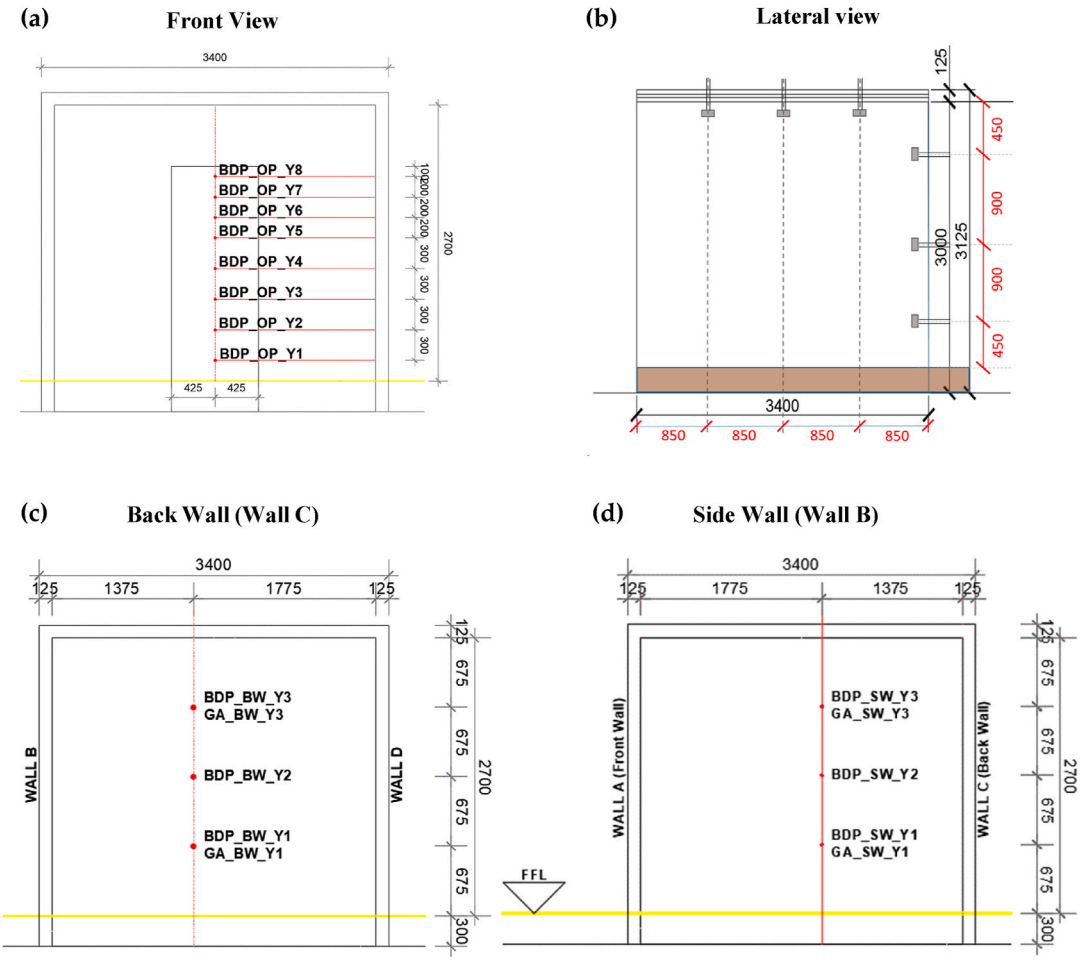

Fig. 12. Location of the velocity probes (a) at the opening of the compartment and (b) within the compartment near the centreline of the ceiling and a lateral wall (ceiling DPT probes only applied in Test 1.2) (c–d) Front view of the location of velocity probes (marked as 'BDP') and gas analyser sampling probes (marked as 'GA') within the compartment. The measuring points were located 300 mm away from the compartment boundaries.

lateral wall. The locations of the velocity probes inside the compartment are shown in Fig. 12.

4.6.5. *In-depth temperature measurements*

Thermocouples were placed in-depth at 100 locations spread around the side and rear compartment walls and the ceiling (represented by the

blue circles in Fig. 9b1 and b3). At each of these 25 locations per surface, at least one thermocouple was positioned to measure the temperature either at the plasterboard-CLT interface (for encapsulated surfaces) or at the glue line between the first and second lamellae (for exposed surfaces). On each surface, five of the locations (represented by the larger blue circles) had a number of additional thermocouples, depending on whether they were encapsulated or exposed timber surfaces. On encapsulated surfaces, one additional thermocouple was placed between the plasterboard layers at each of the five locations, while an additional seven thermocouples were placed at various depths through the CLT in each of the corresponding locations on exposed surfaces. The different configurations of in-depth thermocouple placements, including their depth from the fire-exposed surface, are shown in Fig. 13. Where multiple thermocouples were clustered in one location, they were arranged in a circle such that there was a minimum spacing of 30 mm between each—following the recommendation of Reszka [99] to avoid nearby thermocouples disturbing each other. Each thermocouple was placed in a hole drilled by a CNC machine with a stepped drill-bit, such that the final 5 mm at the internal end of each hole was 1.5 mm diameter, while the remainder of the hole was 2 mm diameter. All of the in-depth thermocouples were 1.5 mm diameter MIMS type K thermocouples with insulated junctions, chosen for durability and to ensure a tight fit and precise placement of the tip at the end of each hole.

These measurements allowed the identification of regions experiencing failure, as well as heat transfer, pyrolysis or charring rate analyses at the solid compartment boundaries. The variation of thermocouple setup resulted in a different number of in-depth thermocouples used between tests. With no CLT exposed, two CLT walls exposed and three CLT walls exposed, the number of in-depth thermocouples were 120, 180 and 210, respectively.

Most of the in-depth readings developed in these tests were obtained by drilling from the back of the panels—perpendicular to the heated surface. This technique induces significant errors in temperature measurements [100,101] and in charring rates derived from these [102]. However, inserting thermocouples parallel to the heated surface was not feasible at such a large scale due to the distance of the measuring points from the sides of the panels. Nevertheless, even with some error in the absolute measurement values, temperatures measured in this manner can still be used to identify failure times and phenomena associated with inflexions in temperature evolutions. Proposed correction methods [100–102] also offer the potential for more accurate estimates of in-depth temperatures and charring rates.

4.6.6. Gas species concentrations

A series of four gas sampling lines were installed in the compartment and attached to bespoke gas analysers. The intent of these devices was to analyse the ventilation condition during the development of the fire, and the role of different fuels in the emissions. The bespoke gas analysers consisted of an electrochemical oxygen cell AO2 from Citicel® to measure oxygen concentration and a Non-Dispersive Infrared Spectrometer (NDIR) model 7911 from Crestline Instruments, Inc to measure carbon dioxide, carbon monoxide and unburned hydrocarbons. Using a KNF pump from JAVAC, a flow of 1.5 L/min was sent through a filter system made with glass fibre and a drying system consisting of a bottle with Drierite™ (calcium sulfate).

The sampling lines consisted of stainless steel tubing attached to PVC tubing using a pressure fitting. The suction points of the gas sampling lines were placed 300 mm away from the walls in the locations shown in Fig. 12 (c & d). The suction points were set up near bi-directional velocity probes and at least one gas-phase thermocouple.

4.6.7. Video imaging

External video cameras and a water-cooled GoPro [103] were used to obtain visual observations of the conditions within and external to the compartment. Two video cameras were set up outside the compartment. One was set up directly in front of the compartment opening, which was

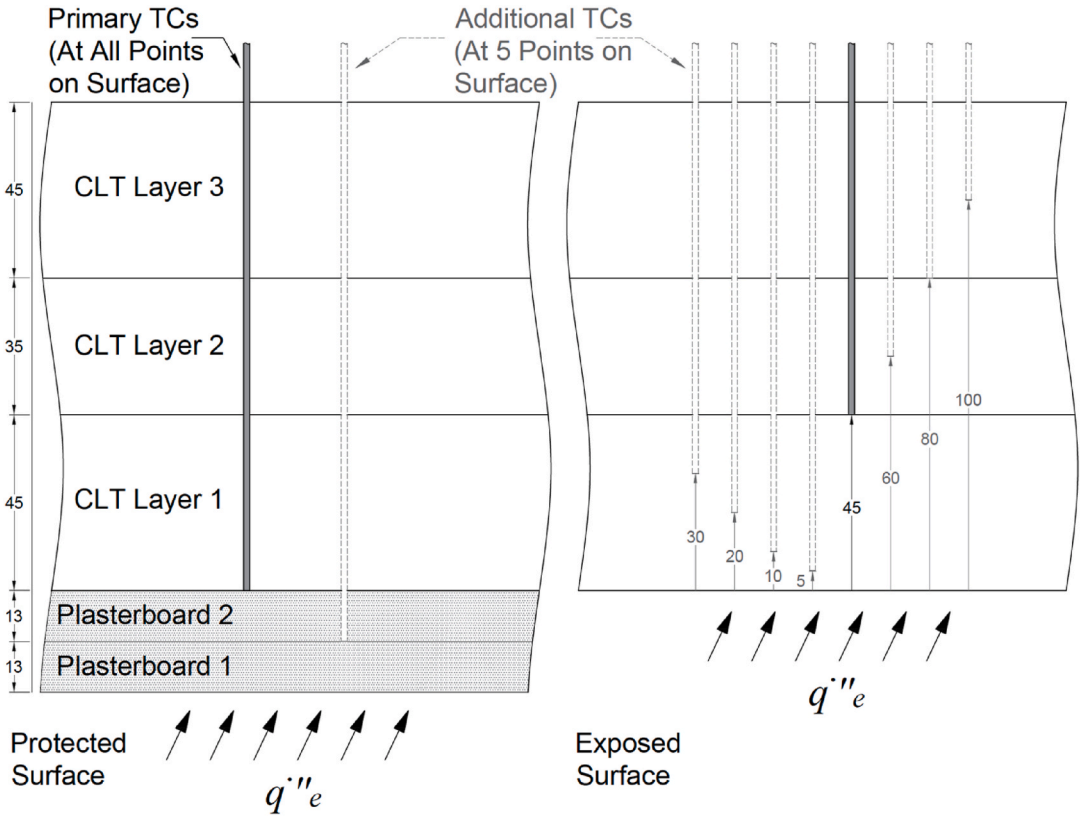

Fig. 13. Placements of in-depth thermocouple measuring points for encapsulated and exposed walls/ceiling.

approximately aligned with the compartment opening centreline. The other one was set up at the side of the compartment, which was approximately aligned with the outer surface of the compartment front wall to capture the behaviour of the externally venting plume from the side.

The water-cooled GoPro was set up inside a Pyrex® beaker, which has higher heat resistance than regular glass. A water inlet was used to provide cold water into the beaker to maintain the camera and the beaker at a relatively low temperature during the test, while the warmed-up water flows naturally from the edge of the beaker. A metal piece was glued to the front edge (around ¼ of the parimeter) of the beaker to prevent water from flowing from the front of the beaker in order to provide a clear vision for the GoPro. A plasterboard encasing and extra aluminium tape and foil were used for protecting the setup from radiative heat.

4.7. Testing facilities

The compartments were built and tested at the Live Fire Campus at the Whyte Island facilities of the Queensland Fire and Emergency Services in Brisbane (Australia).

5. Summary

Research to date has consolidated the fundamental principles of flaming self-extinction of wood at the material scale. In engineering terms, self-extinction can be quantified based on an external heat flux threshold, leading to self-extinction after a transient period in the thermal and burning behaviour. External heat flux acts as an engineering surrogate for the critical mass loss rate or the non-dimensional mass transfer (B) and Damköhler (Da) numbers.

Multiple authors have developed a number of fire experiments at the compartment scale with different compartment parameters, but primarily 'small compartments'. This body of work has shown interdependent, complex phenomena that can influence the occurrence of self-extinction of engineered timber structures. Time-dependent phenomena include encapsulation failure and char fall-off that lead to increased burning resulting in enhanced thermal feedback (incident heat flux) to the timber structure; and the nature and density of the movable fuel load, which determines the fire severity and burnout duration. The time-independent phenomenon refers to thermal feedback as a function of the configuration of timber exposure and ventilation.

Despite the research efforts on particular parameters affecting the self-extinction of CLT, a framework to address design for self-extinction based on a systematic testing campaign is not available. This paper has introduced a methodology based on a series of six large-scale tests (demonstrators) to develop and validate a self-extinction framework based on a study of time-scale conditions (encapsulation failure and char fall-off), the thermal feedback condition, and the fuel load nature (charring and non-charring). The test series were heavily instrumented to characterise each of these phenomena and were designed to isolate individual phenomena. Studies focused on the plasterboard failure and char fall-off were developed by controlling the characteristic time for burnout using a pool fire system such that these failure mechanisms were induced or prevented in pairs of configurations. Instead, the study focused on the thermal feedback used a fixed fuel load density (burnout duration of movable fuel load) in two tests with a different configuration of CLT exposure (two vs three exposed surfaces). Finally, the study focused on the fuel load nature by using fuels with a different B number and the same fuel load density (a kerosene pool and a wood crib).

Author statement

Hangyu Xu: Methodology, Formal analysis, Investigation, Writing - Original Draft, Visualization, Project administration.

Ian Pope: Methodology, Investigation, Visualization, Writing - Review & Editing.

Vinny Gupta: Methodology, Investigation, Visualization, Writing - Review & Editing.

Jaime Cadena: Investigation.

Jeronimo Carrascal: Methodology, Investigation, Visualization, Writing - Review & Editing.

David Lange: Writing - Review & Editing.

Martyn S. McLaggan: Writing - Review & Editing.

Julian Mendez: Investigation, Visualization, Writing - Review & Editing.

Andrés Osorio: Methodology, Investigation, Writing - Review & Editing.

Angela. Solarte: Methodology, Investigation, Writing - Review & Editing.

Diana Soriguer: Methodology, Investigation, Writing - Review & Editing.

Jose L. Torero: Funding acquisition, Writing - Review & Editing.

Felix Wiesner: Methodology, Investigation, Writing - Review & Editing.

Abdulrahman Zaben: Methodology, Investigation.

Juan P. Hidalgo: Conceptualization, Supervision, Project administration, Funding acquisition.

Declaration of competing interest

The authors declare that they have no known competing financial interests or personal relationships that could have appeared to influence the work reported in this paper.

Acknowledgements

This project was funded by the ARC Future Timber Hub (IH150100030) and received generous support by QFES, XLam, Hyne Timber, Lend Lease, Knauf and Rockwool International A/S. The authors are extremely grateful to QFES for providing their research facility and engagement with the project. Dr Wiesner is supported by the National Centre for Timber Durability and Design Life. The authors are also thankful for technical guidance for the calorimeter design from Nathan White (CSIRO). Staff and students helping with the project are gratefully acknowledged: A. Bolanos, A. Browning, E. Candansayar, P. Chowdhury, J. Cuevas, C. Gorska, M. Griffith, M. Hewitt, T. Iturralde, M. Javidnejad, G. Kanellopoulos, A. Lucherini, C. Maluk, S. Matthews, L. Ramadhan, D. Tanudirdjo, W. Wu, H. Wyn, YH. Zhang and YS. Zhu.

References

[1] M.H. Ramage, H. Burridge, M. Busse-Wicher, G. Fereday, T. Reynolds, D.U. Shah, G. Wu, L. Yu, P. Fleming, D. Densley-Tingley, J. Allwood, P. Dupree, P.F. Linden, O. Scherman, The wood from the trees: the use of timber in construction, Renew. Sustain. Energy Rev. (2017), https://doi.org/10.1016/j.rser.2016.09.107.

[2] P.D. Kremer, M.A. Symmons, Mass timber construction as an alternative to concrete and steel in the Australia building industry: a PESTEL evaluation of the potential, Int. Wood Prod. J. 6 (2015) 138–147, https://doi.org/10.1179/2042645315Y.0000000010.

[3] C. Cristescu, D. Honfi, K. Sandberg, Y. Sandin, E. Shotton, S.J. Walsh, M. Cramer, D. Ridley, M. De Arana-fernández, D.F. Llana, M.G. Barbero, B. Nasiri, Ž. Krofl, Design for Deconstruction and Reuse of Timber Structures – State of the Art Review Design for Deconstruction and Reuse of Timber Structures – State of the Art Review, 2020, https://doi.org/10.23699/bh1w-zn97.

[4] United Nations General Assembly, Transforming Our World, The 2030 Agenda for Sustainable Development, 2015.

[5] A. Cowlard, A. Bittern, C. Abecassis-Empis, J.L. Torero, others, Some considerations for the fire safe design of tall buildings, Int. J. High-Rise Build. 2 (2013) 63–77.

[6] BS EN 13501-1, Fire Classification of Construction Products and Building Elements. Classification Using Data from Reaction to Fire Tests, 2018, 2018.

[7] BS EN 13501-2, Fire Classification of Construction Products and Building Elements. Classification Using Data from Fire Resistance Tests, excluding ventilation services, 2016 (n.d.) 2016.

[8] Australian Building Codes Board, National Construction Code Volume One Amendement, 1, 2019.

[9] WoodSolutions, WS38-2016 Fire Safety Design of Mid-rise Timber Buildings Basis for the 2016 Changes to the National Construction Code, 2016.
[10] International Code Council, International Building Code, IBC), 2018, 2017.
[11] International Code Council, International Building Code, IBC), 2021, 2020.
[12] International Code Council, International Fire Code, IFC), 2021, 2020.
[13] B. Showalter, Tall mass timber provisions represent historic new building code requirements, Build. Saf. J. (2020).
[14] C. Gorska, J.P. Hidalgo, J.L. Torero, Fire dynamics in mass timber compartments, Fire Saf. J. (2020) 103098, https://doi.org/10.1016/j.firesaf.2020.103098.
[15] C. Gorska, J.P. Hidalgo, Fire safety risks in buildings with exposed mass timber structures, in: IRG49 Sci. Conf. Wood Prot., 2018. Johannesburg South Africa.
[16] J. Su, P.-S. Lafrance, M. Hoehler, M. Bundy, Fire Safety Challenges of Tall Wood Buildings – Phase 2: Task 2 & 3 – Cross Laminated Timber Compartment Fire Tests, 2018.
[17] J. Su, P. Leroux, P.-S. Lafrance, R.G. Berzins, E. Gibbs Karl, M. Weinfurter, Fire Testing of Rooms with Exposed Wood Surfaces in Encapsulated Mass Timber Construction, 2018, https://doi.org/10.4224/23004642.
[18] International Code Council, International Building Code, IBC), 2015, 2015.
[19] B. Östman, D. Brandon, H. Frantzich, Fire safety engineering in timber buildings, Fire Saf. J. 91 (2017) 11–20, https://doi.org/10.1016/j.firesaf.2017.05.002.
[20] A. Law, R. Hadden, We need to talk about timber: fi re safety design in tall buildings, Struct. Eng. (2020) 6.
[21] T.J. Ohlemiller, Smouldering combustion, chapter 9; section 2, in: P.J. DiNenno, D. Drysdale, C.L. Beyler, W.D. Walton (Eds.), SFPE Handb. Fire Prot. Eng., third ed., 2002, pp. 2–200.
[22] F. Wiesner, A. Bartlett, S. Mohaine, F. Robert, R. McNamee, J.C. Mindeguia, L. Bisby, Structural capacity of one-way spanning large-scale cross-laminated timber slabs in standard and natural fires, Fire Technol. 57 (2021) 291–311, https://doi.org/10.1007/s10694-020-01003-y.
[23] V. Babrauskas, Ignition of wood: a review of the state of the art, J. Fire Protect. Eng. (2002), https://doi.org/10.1177/10423910260620482.
[24] P. Reszka, J.L. Torero, Fire behavior of timber and lignocellulose, in: M. Naceur Belgacem, A. Pizzi (Eds.), Lignocellul. Fibers Wood Handb. Renew. Mater. Today's Environ., Wiley, 2016, pp. 555–578.
[25] C.H.J. Bamford, L. Crank, D.H. Malan, The combustion of wood, part 1, Cambridge Philos. Soc. Proc. Biol. Sci. 42 (1946) 166–182.
[26] A. Tewarson, R.F.F. Pion, Flammability of plastics—I. Burning intensity, Combust. Flame 26 (1976) 85–103, https://doi.org/10.1016/0010-2180(76)90059-6.
[27] R.V. Petrella, The mass burning rate and mass transfer number of selected polymers, wood, and organic liquids, Polym. Plast. Technol. Eng. 13 (1979) 83–103, https://doi.org/10.1080/03602557908067676.
[28] D.J. Rasbash, D.D. Drysdale, D. Deepak, Critical heat and mass transfer at pilot ignition and extinction of a material, Fire Saf. J. 10 (1986) 1–10, https://doi.org/10.1016/0379-7112(86)90026-3.
[29] F.A. Williams, Combustion Theory, CRC Press, 2018, https://doi.org/10.1201/9780429494055.
[30] J.L. Torero, Flaming ignition of solids fuels, in: M.J. Hurley, D. Gottuk, J.R. Hall, K. Harada, E. Kuligowski, M. Puchovsky, J. Torero, J.M. Watts, C. Wieczorek (Eds.), SFPE Handb. Fire Prot. Eng., fifth ed., Springer New York, New York, NY, 2016 https://doi.org/10.1007/978-1-4939-2565-0.
[31] D.B. Spalding, The combustion of liquid fuels, Symp. Combust. 4 (1953) 847–864, https://doi.org/10.1016/S0082-0784(53)80110-4.
[32] J.L. Torero, T. Vietoris, G. Legros, P. Joulain, Estimation of a total mass transfer number from the standoff distance of a spreading flame, Combust. Sci. Technol. 174 (2002) 187–203, https://doi.org/10.1080/713712953.
[33] H.W. Emmons, The film combustion of liquid fuel, ZAMM - Zeitschrift Für Angew. Math. Und Mech. 36 (1956) 60–71, https://doi.org/10.1002/zamm.19560360105.
[34] V. Gupta, J.L. Torero, J.P. Hidalgo, Burning dynamics and in-depth flame spread of wood cribs in large compartment fires, Combust. Flame 228 (2021) 42–56, https://doi.org/10.1016/j.combustflame.2021.01.031.
[35] A. Bartlett, R. Hadden, L. Bisby, B. Lane, Auto-extinction of Engineered Timber: the Application of Firepoint Theory, Interflam, 2016.
[36] R. Emberley, A. Inghelbrecht, Z. Yu, J.L. Torero, Self-extinction of timber, Proc. Combust. Inst. 36 (2017) 3055–3062, https://doi.org/10.1016/j.proci.2016.07.077.
[37] R. Emberley, T. Do, J. Yim, J.L. Torero, Critical heat flux and mass loss rate for extinction of flaming combustion of timber, Fire Saf. J. 91 (2017) 252–258, https://doi.org/10.1016/j.firesaf.2017.03.008.
[38] S.M. Arnórsson, R.M. Hadden, A. Law, The variability of critical mass loss rate at auto-extinction, Fire Technol. 57 (2021) 233–246, https://doi.org/10.1007/s10694-020-01002-z.
[39] M. Spearpoint, J. Quintiere, Predicting the burning of wood using an integral model, Combust. Flame 123 (2000) 308–325, https://doi.org/10.1016/S0010-2180(00)00162-0.
[40] J. Cuevas, J.L. Torero, C. Maluk, Flame extinction and burning behaviour of timber under varied oxygen concentrations, Fire Saf. J. (2020) 103087, https://doi.org/10.1016/j.firesaf.2020.103087.
[41] J.P. Hidalgo, P. Pironi, R.M. Hadden, S. Welch, Effect of thickness on the ignition behaviour of carbon fibre composite materials used in high pressure vessels, in: 8th Int. Semin. Fire Explos. Hazards, 2016, https://doi.org/10.20285/c.sklfs.8thISFEH.036. Hefei, China.
[42] C. Lautenberger, C. Fernandez-Pello, A model for the oxidative pyrolysis of wood, Combust. Flame 156 (2009) 1503–1513, https://doi.org/10.1016/j.combustflame.2009.04.001.
[43] BS EN 1363-1, Fire Resistance Tests — Part 1, General Requirements, 2012.
[44] A.I. Bartlett, R.M. Hadden, J.P. Hidalgo, S. Santamaria, F. Wiesner, L.A. Bisby, S. Deeny, B. Lane, Auto-extinction of engineered timber: application to compartment fires with exposed timber surfaces, Fire Saf. J. 91 (2017) 407–413, https://doi.org/10.1016/j.firesaf.2017.03.050.
[45] A. Cowlard, A. Bittern, C. Abecassis-Empis, J. Torero, Fire Safety Design for Tall Buildings, Procedia Eng., 2013, pp. 169–181, https://doi.org/10.1016/j.proeng.2013.08.053.
[46] R. Emberley, C.G. Putynska, A. Bolanos, A. Lucherini, A. Solarte, D. Soriguer, M. G. Gonzalez, K. Humphreys, J.P. Hidalgo, C. Maluk, A. Law, J.L. Torero, Description of small and large-scale cross laminated timber fire tests, Fire Saf. J. (2017), https://doi.org/10.1016/j.firesaf.2017.03.024.
[47] C. McGregor, Contribution of Cross Laminated Timber Panels to Room Fires, Carleton University, 2013.
[48] A.R. Medina Hevia, Fire Resistance of Partially Protected Cross-Laminated Timber Rooms, Carleton University, 2014.
[49] S. Nothard, D. Lange, J.P. Hidalgo, V. Gupta, M.S. McLaggan, The response of exposed timber in open plan compartment fires and its impact on the fire dynamics, in: Proc. 11th Int. Conf. Struct. Fire, The University of Queensland, Brisbane, Australia, 2020, https://doi.org/10.14264/5d97785.
[50] C. Gorska, Fire Dynamics in Multi-Scale Timber Compartments, The University of Queensland, 2020, https://doi.org/10.14264/uql.2020.795.
[51] R.M. Hadden, A.I. Bartlett, J.P. Hidalgo, S. Santamaria, F. Wiesner, L.A. Bisby, S. Deeny, B. Lane, Effects of exposed cross laminated timber on compartment fire dynamics, Fire Saf. J. (2017), https://doi.org/10.1016/j.firesaf.2017.03.074.
[52] D. Brandon, C. Dagenais, Fire Safety Challenges of Tall Wood Buildings – Phase 2: Task 5 – Experimental Study of Delamination of Cross Laminated Timber (CLT) in Fire, 2018.
[53] E. Johansson, A. Svenningsson, Delamination of Cross-Laminated Timber and its Impact on Fire Development: Focusing on Different Types of Adhesives, 2018. Lund.
[54] A. Frangi, M. Fontana, A. Mischler, Shear behaviour of bond lines in glued laminated timber beams at high temperatures, Wood Sci. Technol. 38 (2004) 119–126, https://doi.org/10.1007/s00226-004-0223-y.
[55] P. Chowdhury, Experimental Study of Char Fall-Off Phenomenon in CLT under Fire, The University of Queensland, 2019.
[56] L. Schmidt, Experimental Study on the Effect of Char Fall off on the Heat Transfer within Loaded Cross-Laminated Timber Columns Exposed to Radiant Heating, The University of Edinburgh, 2020.
[57] S.L. Zelinka, K. Sullivan, S. Pei, N. Ottum, N.J. Bechle, D.R. Rammer, L. E. Hasburgh, Small scale tests on the performance of adhesives used in cross laminated timber (CLT) at elevated temperatures, Int. J. Adhesion Adhes. 95 (2019), https://doi.org/10.1016/j.ijadhadh.2019.102436.
[58] S. Clauß, M. Joscak, P. Niemz, Thermal stability of glued wood joints measured by shear tests, Eur. J. Wood Wood Prod. 69 (2011) 101–111, https://doi.org/10.1007/s00107-010-0411-4.
[59] J. Konnerth, M. Kluge, G. Schweizer, M. Miljković, W. Gindl-Altmutter, Survey of selected adhesive bonding properties of nine European softwood and hardwood species, Eur. J. Wood Wood Prod. 74 (2016) 809–819, https://doi.org/10.1007/s00107-016-1087-1.
[60] M. Klippel, Fire Safety of Bonded Structural Timber Elements, ETH ZURICH, 2014.
[61] F. Wiesner, D. Thomson, L. Bisby, The effect of adhesive type and ply number on the compressive strength retention of CLT at elevated temperatures, Construct. Build. Mater. 266 (2021) 121156, https://doi.org/10.1016/j.conbuildmat.2020.121156.
[62] F. Wiesner, S. Deeny, L.A. Bisby, Influence of ply configuration and adhesive type on cross-laminated timber in flexure at elevated temperatures, Fire Saf. J. (2020) 103073, https://doi.org/10.1016/j.firesaf.2020.103073.
[63] F. Wiesner, Structural Behaviour of Cross-Laminated Timber Elements in Fires, The University of Edinburgh, 2019.
[64] D.I. Kolaitis, E.K. Asimakopoulou, M.A. Founti, Fire protection of light and massive timber elements using gypsum plasterboards and wood based panels: a large-scale compartment fire test, Construct. Build. Mater. 73 (2014) 163–170, https://doi.org/10.1016/j.conbuildmat.2014.09.027.
[65] A. Lucherini, Q.S. Razzaque, C. Maluk, Exploring the fire behaviour of thin intumescent coatings used on timber, Fire Saf. J. 109 (2019) 102887, https://doi.org/10.1016/j.firesaf.2019.102887.
[66] D. Barber, Fire safety of mass timber buildings with CLT in USA, Wood Fiber Sci. 50 (2018) 83–95.
[67] J.P. Hidalgo, S. Welch, J.L. Torero, Performance criteria for the fire safe use of thermal insulation in buildings, Construct. Build. Mater. 100 (2015) 285–297, https://doi.org/10.1016/j.conbuildmat.2015.10.014.
[68] Structural Timber Association, Structural timber buildings fire safety in use guidance Volume 6 - mass timber structures, in: Building Regulation Compliance B3, 2020, 1.
[69] P.H. Thomas, A.J. Heselden, M. Law, Fully-developed Compartment Fires - Two Kinds of Behaviour, 1967. London, UK.
[70] P.H. Thomas, A.J.M. Heselden, Fully-developed Fires in Single Compartments, A Co-operative Research Programme of the Conseil International Du Bâtiment, 1972.
[71] J.L. Torero, A.H. Majdalani, A.E. Cecilia, A. Cowlard, Revisiting the compartment fire, Fire Saf. Sci. 11 (2014) 28–45, https://doi.org/10.3801/IAFSS.FSS.11-28.
[72] S.E. Magnusson, S. Thelandersson, Temperature-time curves of complete process of fire development, Bull. Div. Struct. Mech. Concr. Constr. Bull. 16 (1970).

[73] U. Wickström, Application of the standard fire curve for expressing natural fires for design purposes, in: T. Harmathy (Ed.), Fire Saf. Sci. Eng., ASTM International, 100 Barr Harbor Drive, PO Box C700, West Conshohocken, PA 19428-2959, 1985, p. 145, https://doi.org/10.1520/STP35295S. -145–15.
[74] J. Franssen, Improvement of the parametric fire of Eurocode 1 based on experimental test results, Fire Saf. Sci. 6 (2000) 927–938, https://doi.org/10.3801/IAFSS.FSS.6-927.
[75] European Standard, EN 1991-1-2 Eurocode 1: Actions on Structures - Part 1-2: General Actions - Actions on Structures Exposed to Fire, 2002.
[76] T. Lennon, D. Moore, The natural fire safety concept—full-scale tests at Cardington, Fire Saf. J. 38 (2003) 623–643, https://doi.org/10.1016/s0379-7112(03)00028-6.
[77] J.-C. Gerardy, Sustainable steel buildings through natural safety concept, in: CBTUH 2008 8th World Congr., Dubai, 2008.
[78] V. Gupta, Open-plan Compartment Fire Dynamics, The University of Queensland, 2021. https://doi.org/10.14264/d35999e.
[79] D. Brandon, J. Anderson, Wind effect on internal and external compartment fire exposure, RISE Rep. 72 (2018), 2018.
[80] S.L. Zelinka, L.E. Hasburgh, K.J. Bourne, D.R. Tucholski, J.P. Ouellette, Compartment Fire Testing of a Two-Story Mass Timber Building, 2018.
[81] D. Brandon, J. Sjöström, E. Hallberg, A. Temple, F. Kahl, Fire Safe Implementation of Mass Timber in Tall Buildings, 2021. https://www.ri.se/en/what-we-do/projects/fire-safe-implementation-of-mass-timber-in-tall-buildings.
[82] A. Just, D. Brandon, K.N. Mäger, R. Pukk, CLT compartment fire test, in: 2018 World Conf. Timber Eng., 2018. Seoul, Republic of Korea.
[83] M. Janssens, A. Joyce, Development of a fire performance assessment method for qualifying cross-laminated timber adhesives, in: Proc. 15th Int. Interflam Conf., Interscience Communications Ltd., Royal Holloway College University of London, UK, 2019.
[84] T. Harmathy, Experimental study on the effect of ventilation on the burning of piles of solid fuels, Combust. Flame 31 (1978) 259–264, https://doi.org/10.1016/0010-2180(78)90138-4.
[85] T. Harmathy, Mechanism of burning of fully-developed compartment fires, Combust. Flame 31 (1978) 265–273, https://doi.org/10.1016/0010-2180(78)90139-6.
[86] A. Browning, The Effect of Fuel Load Nature on the Self-Extinction of Mass Timber, The University of Queensland, 2018.
[87] N. Tondini, J.M. Franssen, Analysis of experimental hydrocarbon localised fires with and without engulfed steel members, Fire Saf. J. 92 (2017) 9–22, https://doi.org/10.1016/j.firesaf.2017.05.011.
[88] XLam Australia Pty Ltd, XLam Australian Cross Laminated Timber Panel Structural Guide, 2017.
[89] J.P. Hidalgo, T. Goode, V. Gupta, A. Cowlard, C. Abecassis-Empis, J. Maclean, A. I. Bartlett, C. Maluk, J.M. Montalvá, A.F. Osorio, J.L. Torero, The Malveira fire test: full-scale demonstration of fire modes in open-plan compartments, Fire Saf. J. 108 (2019) 102827, https://doi.org/10.1016/j.firesaf.2019.102827.
[90] Australia Standards, AS/NZS 1080.1:2012 Timber-Methods of Test - Method 1: Moisture Content, 2012.
[91] BS EN ISO 1716, Reaction to Fire Tests for Products — Determination of the Gross Heat of Combustion (Calorific Value), 2010.
[92] N. White, H. Xu, J. Abraham, J. Carrascal, J.P. Hidalgo, V. Gupta, N. Weerakkody, Buoyancy-driven calorimeter for post-flashover heat release rate measurements, in: 12th Asia-Oceania Symp, Fire Sci. Technol., Brisbane, Australia, 2021.
[93] M. Shipp, M. Spearpoint, Measurements of the severity of fires involving private motor vehicles, Fire Mater. 19 (1995) 143–151, https://doi.org/10.1002/fam.810190307.
[94] British Standards Institution, BS ISO 5660-1, Reaction-to-fire Tests — Heat Release , Smoke Production and Mass Loss Rate. Part 1 : Heat Release Rate (Cone Calorimeter Method) and Smoke Production Rate (Dynamic Measurement), 2015, p. 66pp, 2015.
[95] H. Biteau, T. Steinhaus, C. Schemel, A. Simeoni, G. Marlair, N. Bal, J. Torero, Calculation methods for the heat release rate of materials of unknown composition, Fire Saf. Sci. 9 (2008) 1165–1176, https://doi.org/10.3801/IAFSS.FSS.9-1165.
[96] J.P. Hidalgo, C. Maluk, A. Cowlard, C. Abecassis-Empis, M. Krajcovic, J.L. Torero, A Thin Skin Calorimeter (TSC) for quantifying irradiation during large-scale fire testing, Int. J. Therm. Sci. 112 (2017) 383–394, https://doi.org/10.1016/j.ijthermalsci.2016.10.013.
[97] B. McCaffrey, G. Heskestad, B. McCaffrey Heskestad G, A robust bidirectional low-velocity probe for flame and fire applications, Combust. Flame 26 (1976) 125–127. http://fire.nist.gov/bfrlpubs/fire76/PDF/f76002.pdf. (Accessed 10 May 2013).
[98] V. Gupta, J.L. Torero, C. Maluk, J.P. Hidalgo, Analysis of convective heat losses in a full-scale compartment fire experiment, in: 9th Int. Semin. Fire Explos. Hazards, 2019, https://doi.org/10.18720/SPBPU/2/k19-53. St. Petersburg, Russia.
[99] P. Reszka, in: In-Depth Temperature Profiles in Pyrolyzing Wood, The University of Edinburgh, 2008.
[100] J.V. Beck, Thermocouple temperature disturbances in low conductivity materials, J. Heat Tran. 84 (1962) 124, https://doi.org/10.1115/1.3684310.
[101] I. Pope, J.P. Hidalgo, R.M. Hadden, J.L. Torero, A simplified correction method for thermocouple disturbance errors in solids, Int. J. Therm. Sci. 172 (A) (2022) 107324, https://doi.org/10.1016/j.ijthermalsci.2021.107324.
[102] I. Pope, J.P. Hidalgo, J.L. Torero, A correction method for thermal disturbances induced by thermocouples in a low-conductivity charring material, Fire Saf. J. 120 (2021) 103077, https://doi.org/10.1016/j.firesaf.2020.103077.
[103] M. Hoehler, Improved Video Capture for Severe Fire Environments, NIST-Internal Present, 2020.